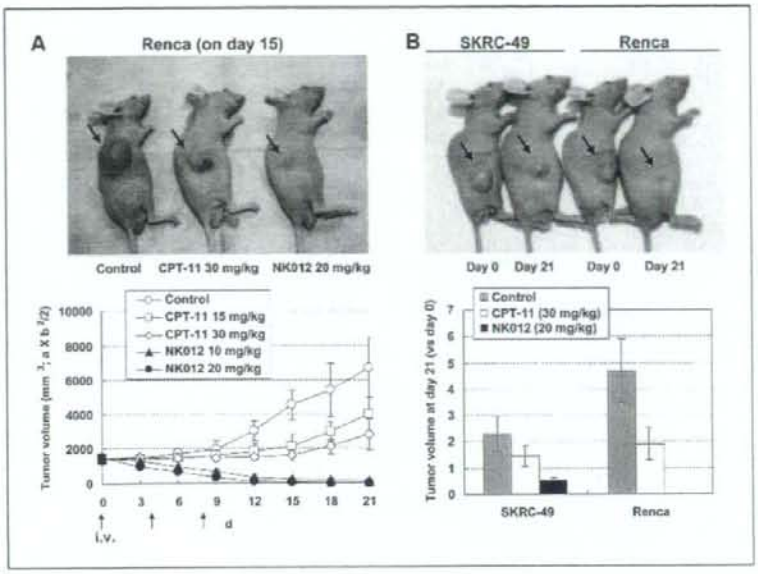

Figure 2. Growth-inhibitory effect of NK012 and CPT-11 on bulky RCC tumors. I.v. administration of NK012 or CPT-11 was started when the mean tumor volumes of groups reached a massive 1,500 mm^3. The mice were divided into test groups as indicated. *A*, representative of each group at day 15 in the Renca allograft model. *Arrows*, Renca allografts (*top*). Time profile of tumor volume in mice treated with NK012 or CPT-11 at indicated doses (*bottom*). Each group consisted of 10 mice. *Bars*, SD. *B*, the comparison of antitumor activities of CPT-11 and NK012 in SKRC-49 xenografts and Renca allografts. Representative of mice treated with NK012 at day 0 and day 21. Experiments were repeated twice with similar results. The mice at day 0 in the photograph belong to the group in the second experiment which started just at day 21 of the first experiment. *Arrows*, tumor grafts. The relative tumor volume values at day 21 to those at day 0 in each group set to 1 (*bottom*). Each group consisted of 10 mice.

Fig. 3*B*). On the other hand, the concentrations of free SN-38 after administration of CPT-11 were almost negligible in metastatic lung tissues at all time points (data not shown). These results strongly suggest that SN-38 could be selectively released from NK012 and maintained in metastatic Renca tumor tissues.

Deviating from the ordinary experimental pulmonary metastasis prevention model, we initiated treatment 7 days after inoculation (day 0) when multiple lung nodules derived from Renca were observed in all mice in our preliminary study (Fig. 4*A*). On day 21, there was no significant difference between the mean number of metastatic nodules in the control group (287 ± 56 nodules, $n = 10$) and in the group receiving CPT-11 treatment (236 ± 59 nodules, $n = 10$). Significant treatment effects were found, however, in the group receiving NK012 treatment (32 ± 18 nodules, $n = 10$) on day 21 compared with the control group on day 21 ($P < 0.0001$). Notably, a dramatic decrease in metastatic nodule number was observed in the NK012 treatment group on day 21 compared with the control group on day 0 (126 ± 23 nodules, $n = 10$, $P < 0.001$; Fig. 4*A*). Kaplan-Meier analysis showed that a significant survival benefit was obtained in the NK012 treatment group compared with

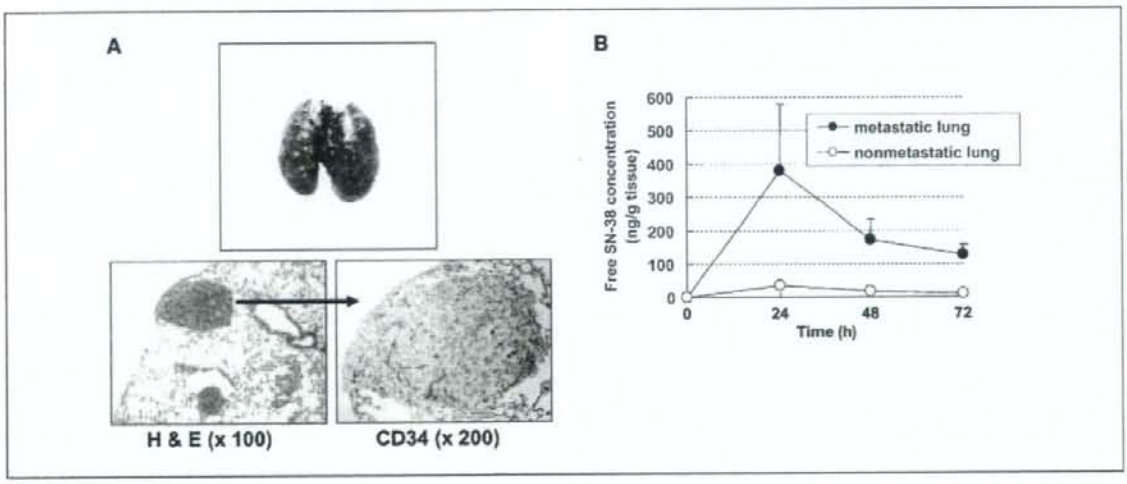

Figure 3. Pulmonary metastasis of Renca cells and lung tissue distribution of free SN-38 after administration of NK012 and CPT-11. *A*, gross appearances of pulmonary metastasis observed 7 d after Renca inoculation (*top*). Multiple metastatic nodules and neovascularization in metastatic lung tumor lesion (*bottom*). *B*, time profile of free SN-38 concentration in metastatic or nonmetastatic lung tissues in mice treated with NK012 (20 mg/kg/d). *Bars*, SD. Experiments were performed in tetraplicate.

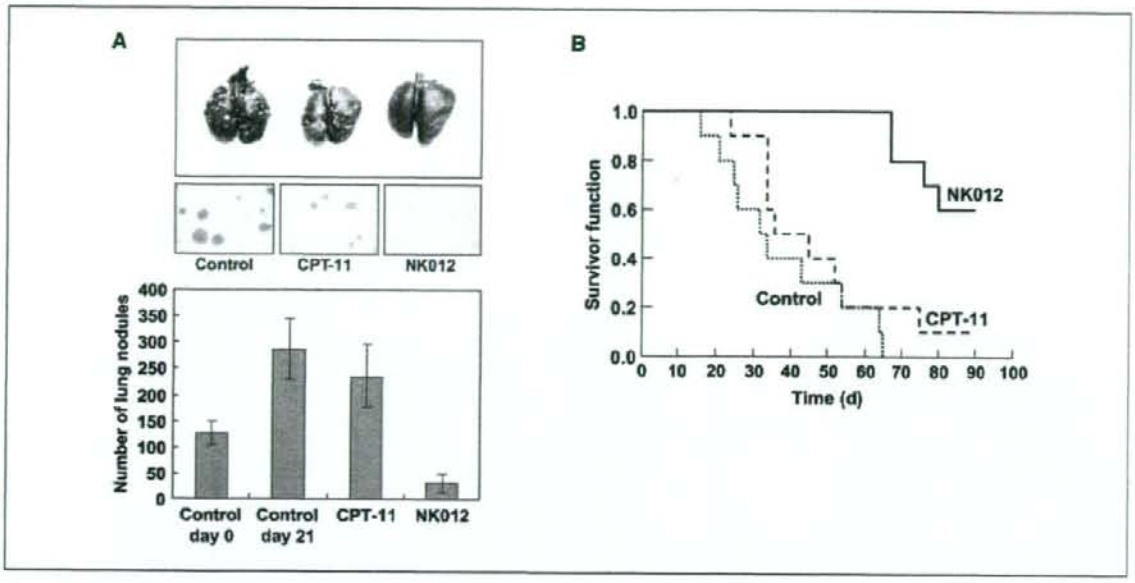

Figure 4. Treatment effect of NK012 on established pulmonary metastasis and survival. NK012 (20 mg/kg/d) and CPT-11 (30 mg/kg/d) were given i.v. to mice with established pulmonary metastasis on days 0 (7 d after Renca inoculation), 4, and 8. *A*, gross and histologic appearances of pulmonary metastases at day 21 (*top*). The metastatic nodules in each mouse were counted. Each group consisted of five mice. *B*, mice were maintained for 90 d after each treatment and survival was assessed by a Kaplan-Meier analysis. Each group consisted of five mice. Experiments were repeated twice with similar results.

the control group ($P < 0.001$), but no significant survival benefit was obtained in CPT-11 treatment group ($P = 0.239$; Fig. 4*B*). Although no severe toxic effects were observed in any mouse treated with NK012, 3 of 10 mice treated with NK012 were sacrificed during the observation period according to the 'Guidelines for Animal Experiments because their body weights had become 10% lower than those of the other mice. However, the sacrificed mice were a little bit smaller than others when they started treatment, and they showed no disseminated lung metastasis (data not shown).

Our results presented here strongly support recent findings reported by us that the macromolecular drug distribution throughout the tumor site was enhanced by the hypervascularity and hyperpermeability, and subsequently higher antitumor activity was achieved (6). We assume that conventional low molecular size anticancer agents almost disappear from the bloodstream without being subjected to the EPR effect before they can reach the target organs (solid tumor). The clinical importance of angiogenesis in human tumors has been shown in several reports indicating a positive relationship between the blood vessel density in the tumor mass and poor prognosis with chemoresistance in patients with various cancers (7–9). Furthermore, recent reports showing that anticancer agents were less active against VEGF-overexpressing tumors (10, 11) may support the idea that low-molecular drugs are not so effective in the treatment of solid tumors which are rich in blood vessels.

Our study thus far has several limitations about clarifying whether extensive angiogenesis in the tumor is an essential determinant for the susceptibility to NK012. In our ongoing study, we found that NK012 also has a striking antitumor activity against some hypovascular tumor models of human pancreatic cancer xenografts.[5] It also remains unclear whether NK012 possesses strong antitumor activity in other metastatic sites besides the lung. It is known that the EPR effect is affected by various permeability factors, such as bradykinin (12), nitric oxide (13), and various cytokines independent of VEGF and hypervascularity (14). Among solid tumors with rapid progression potential, irregularity occurs not only in blood flow and vascular density, but also in the vascular network and anatomic architecture (15, 16), suggesting that EPR effect may be predominantly promoted in rapid-progressive tumor phenotypes and influenced by organ-specific tumor microenvironment. Hoffman and coworkers (17, 18) have developed a technique of surgical orthotopic implantation (SOI) with more clinical features of systemic and aggressive metastases than our conventional animal models. Further preclinical studies using such models as SOI might clarify cancer phenotypes and metastatic organs to which we can apply NK012 more precisely.

The results of chemotherapy in RCCs have been disappointing, as indicated by the low response proportions. However, clinical trials using gemcitabine-containing regimens have been encouraging, with major responses occurring in 5% to 17% of patients (19, 20), suggesting the possibility that chemotherapy is promising as a modality for RCC therapy if anticancer agents can be selectively delivered, released, and maintained around tumor tissues. Our current report highlights the advantages of polymeric micelle-based drug carriers like NK012 as promising modalities for treatment, rather than prevention, of disseminated RCCs with abnormal vascular architecture. The results of our ongoing phase-I

[5] Y. Saito, M. Yasumaga, J. Kuroda, Y. Koga, and Y. Matsumura. Unpublished data.

clinical trial and future phase-II trials of NK012 in patients with advanced solid tumors including RCC might meet or even exceed our expectations.

Acknowledgments

Received 12/10/2007; revised 1/25/2008; accepted 1/31/2008.

Grant support: Grant-in-aid from 3rd Term Comprehensive Control Research for Cancer, Ministry of Health, Labor and Welfare (Y. Matsumura) and Scientific Research on Priority Areas from the Ministry of Education, Culture, Sports, Science and Technology (Y. Matsumura).

The costs of publication of this article were defrayed in part by the payment of page charges. This article must therefore be hereby marked *advertisement* in accordance with 18 U.S.C. Section 1734 solely to indicate this fact.

We thank H. Miyatake and N. Mie for their technical assistance and K. Shiina for her secretarial assistance.

References

1. Matsumura Y, Maeda H. A new concept for macromolecular therapeutics in cancer chemotherapy: mechanism of tumoritropic accumulation of proteins and the antitumor agent smancs. Cancer Res 1986;46:6387–92.
2. Yokoyama M, Miyauchi M, Yamada N, et al. Characterization and anticancer activity of the micelle-forming polymeric anticancer drug adriamycin-conjugated poly(ethylene glycol)-poly(aspartic acid) block copolymer. Cancer Res 1990;50:1693–700.
3. Kataoka K, Harada A, Nagasaki Y. Block copolymer micelles for drug delivery: design, characterization and biological significance. Adv Drug Deliv Rev 2001;47:113–31.
4. Matsumura Y, Hamaguchi T, Ura T, et al. Phase I clinical trial and pharmacokinetic evaluation of NK911, a micelle-encapsulated doxorubicin. Br J Cancer 2004;91:1775–81.
5. Hamaguchi T, Kato K, Yasui H, et al. A phase I and pharmacokinetic study of NK105, a paclitaxel-incorporating micellar nanoparticle formulation. Br J Cancer 2007;97:170–6.
6. Koizumi F, Kitagawa M, Negishi T, et al. Novel SN-38-incorporating polymeric micelles, NK012, eradicate vascular endothelial growth factor-secreting bulky tumors. Cancer Res 2006;66:10048–56.
7. Gasparini G, Harris AL. Clinical importance of the determination of tumor angiogenesis in breast carcinoma: much more than a new prognostic tool. J Clin Oncol 1995;13:765–82.
8. Takahashi Y, Kitadai Y, Bucana CD, Cleary KR, Ellis LM. Expression of vascular endothelial growth factor and its receptor, KDR, correlates with vascularity, metastasis, and proliferation of human colon cancer. Cancer Res 1995;55:3964–8.
9. Williams JK, Carlson GW, Cohen C, Derose PB, Hunter S, Jurkiewicz MJ. Tumor angiogenesis as a prognostic factor in oral cavity tumors. Am J Surg 1994;168:373–80.
10. Natsume T, Watanabe J, Koh Y, et al. Antitumor activity of TZT-1027 (Soblidotin) against vascular endothelial growth factor-secreting human lung cancer *in vivo*. Cancer Sci 2003;94:826–33.
11. Zhang L, Hannay JA, Liu J, et al. Vascular endothelial growth factor overexpression by soft tissue sarcoma cells: implications for tumor growth, metastasis, and chemoresistance. Cancer Res 2006;66:8770–8.
12. Matsumura Y, Maruo K, Kimura M, Yamamoto T, Konno T, Maeda H. Kinin-generating cascade in advanced cancer patients and *in vitro* study. Jpn J Cancer Res 1991;82:732–41.
13. Wu J, Akaike T, Hayashida K, et al. Identification of bradykinin receptors in clinical cancer specimens and murine tumor tissues. Int J Cancer 2002;98:29–35.
14. Maeda H, Fang J, Inutsuka T, Kitamoto Y. Vascular permeability enhancement in solid tumor: various factors, mechanisms involved and its implications. Int Immunopharmacol 2003;3:319–28.
15. Suzuki M, Takahashi T, Sato T. Medial regression and its functional significance in tumor-supplying host arteries. A morphometric study of hepatic arteries in human livers with hepatocellular carcinoma. Cancer 1987;59:444–50.
16. Skinner SA, Tutton PJ, O'Brien PE. Microvascular architecture of experimental colon tumors in the rat. Cancer Res 1990;50:2411–7.
17. An Z, Jiang P, Wang X, Moossa AR, Hoffman RM. Development of a high metastatic orthotopic model of human renal cell carcinoma in nude mice: benefits of fragment implantation compared to cell-suspension injection. Clin Exp Metastasis 1999;17:265–70.
18. Hoffman RM. Orthotopic metastatic mouse models for anticancer drug discovery and evaluation: a bridge to the clinic. Invest New Drugs 1999;17:343–59.
19. Rini BI, Vogelzang NJ, Dumas MC, Wade JL III, Taber DA, Stadler WM. Phase II trial of weekly intravenous gemcitabine with continuous infusion fluorouracil in patients with metastatic renal cell cancer. J Clin Oncol 2000;18:2419–26.
20. Nanus DM, Garino A, Milowsky MI, Larkin M, Dutcher JP. Active chemotherapy for sarcomatoid and rapidly progressing renal cell carcinoma. Cancer 2004;101:1545–51.

Int. J. Cancer: **122,** 2148–2153 (2008)

Synergistic antitumor activity of the novel SN-38-incorporating polymeric micelles, NK012, combined with 5-fluorouracil in a mouse model of colorectal cancer, as compared with that of irinotecan plus 5-fluorouracil

Takako Eguchi Nakajima[1,2], Masahiro Yasunaga[2], Yasuhiko Kano[3], Fumiaki Koizumi[4], Ken Kato[1], Tetsuya Hamaguchi[1], Yasuhide Yamada[1], Kuniaki Shirao[1], Yasuhiro Shimada[1] and Yasuhiro Matsumura[2]*

[1]*Gastrointestinal Oncology Division, National Cancer Center Hospital, Tokyo, Japan*
[2]*Investigative Treatment Division, Research Center for Innovative Oncology, National Cancer Center Hospital East, Kashiwa, Chiba, Japan*
[3]*Hematology Oncology, Tochigi Cancer Center, Tochigi, Japan*
[4]*Shien Lab Medical Oncology Division, National Cancer Center Hospital, Tokyo, Japan*

The authors reported in a previous study that NK012, a 7-ethyl-10-hydroxy-camptothecin (SN-38)-releasing nano-system, exhibited high antitumor activity against human colorectal cancer xenografts. This study was conducted to investigate the advantages of NK012 over irinotecan hydrochloride (CPT-11) administered in combination with 5-fluorouracil (5FU). The cytotoxic effects of NK012 or SN-38 (an active metabolite of CPT-11) administered in combination with 5FU was evaluated *in vitro* in the human colorectal cancer cell line HT-29 by the combination index method. The effects of the same drug combinations was also evaluated *in vivo* using mice bearing HT-29 and HCT-116 cells. All the drugs were administered i.v. 3 times a week; NK012 (10 mg/kg) or CPT11 (50 mg/kg) was given 24 hr before 5FU (50 mg/kg). Cell cycle analysis in the HT-29 tumors administered NK012 or CPT-11 *in vivo* was performed by flow cytometry. NK012 exerted more synergistic activity with 5FU compared to SN-38. The therapeutic effect of NK012/5FU was significantly superior to that of CPT-11/5FU against HT-29 tumors ($p = 0.0004$), whereas no significant difference in the antitumor effect against HCT-116 tumors was observed between the 2-drug combinations ($p = 0.2230$). Cell-cycle analysis showed that both NK012 and CPT-11 tend to cause accumulation of cells in the S phase, although this effect was more pronounced and maintained for a more prolonged period with NK012 than with CPT-11. Optimal therapeutic synergy was observed between NK012 and 5FU, therefore, this regimen is considered to hold promise of clinical benefit, especially for patients with colorectal cancer.

Key words: NK012; SN-38; 5-fluorouracil; drug delivery system; colorectal cancer

The 5-year survival rates of colorectal cancer (CRC) have improved remarkably over the last 10 years, accounted for in large part by the extensively investigated agents after 5-fluorouracil (5FU). Irinoetcan hydrochloride (CPT-11), a water-soluble, semi-synthetic derivative of camptothecin, is one such agent that has been shown to be highly effective, and currently represents a key-drug in first- and second-line treatment regimens for CRC. CPT-11 monotherapy, however, has not been shown to yield superior efficacy, including in terms of the median survival time, to bolus 5FU/leucovorin (LV) alone.[1] In 2 Phase III trials, the addition of CPT-11 to bolus or infusional 5FU/LV regimens clearly yielded greater efficacy than administration of 5FU/LV alone, with a doubling of the tumor response rate and prolongation of the median survival time by 2–3 months.[1,2]

CPT-11 is converted to 7-ethyl-10-hydroxy-camptothecin (SN-38), a biologically active and water-insoluble metabolite of CPT-11, by carboxylesterases in the liver and the tumor. SN-38 has been demonstrated to exhibit up to a 1,000-fold more potent cytotoxic activity than CPT-11 against various cancer cells *in vitro*.[3] The metabolic conversion rate is, however, very low, with only <10% of the original volume of CPT-11 being metabolized to SN-38[4,5]; conversion of CPT-11 to SN-38 also depends on genetic interindividual variability of the activity of carboxylesterases.[6] Direct use of SN-38 itself for clinical cancer treatment must be shown to be identical in terms of both efficacy and toxicity.

Some drugs incorporated in drug delivery systems (DDS), such as Abraxane and Doxil, are already in clinical use.[7,8] The clinical benefits of DDS are based on their EPR effect.[9] The EPR effect is based on the pathophysiological characteristics of solid tumor tissues: hypervascularity, incomplete vascular architecture, secretion of vascular permeability factors stimulating extravasation within cancer tissue, and absence of effective lymphatic drainage from the tumors that impedes the efficient clearance of macromolecules accumulated in solid tumor tissues. Several types of DDS can be used for incorporation of a drug. A liposome-based formulation of SN-38 (LE-SN38) has been developed, and a clinical trial to assess its efficacy is now under way.[10,11]

Recently, we demonstrated that NK012, novel SN-38-incorporating polymeric micelles, exerted superior antitumor activity and less toxicity than CPT-11.[12] NK012 is characterized by a smaller size of the particles than LE-SN38; the mean particle diameter of NK012 is 20 nm. NK012 can release SN-38 under neutral conditions even in the absence of a hydrolytic enzyme, because the bond between SN-38 and the block copolymer is a phenol ester bond, which is stable under acidic conditions and labile under mild alkaline conditions. The release rate of SN-38 from NK012 under physiological conditions is quite high; more than 70% of SN-38 is released within 48 hr. We speculated that the use of NK012, in place of CPT-11, in combination with 5FU may yield superior results in the treatment of CRC. In the present study, we evaluated the antitumor activity of NK012 administered in combination with 5FU as compared to that of CPT-11 administered in combination with 5FU against CRC in an experimental model.

Material and methods

Cells and animals

The human colorectal cancer cell lines used, namely, HT-29 and HCT-116, were purchased from the American Type Culture Collection (Rockville, MD). The HT-29 cells and HCT-116 cells were maintained in RPMI 1640 supplemented with 10% fetal bovine serum (Cell Culture Technologies, Gaggenau-Hoerden, Germany), penicillin, streptomycin, and amphotericin B (100 units/mL, 100 μg/mL, and 25 μg/mL, respectively; Sigma, St. Louis, MO) in a humidified atmosphere containing 5% CO_2 at 37°C.

BALB/c *nu/nu* mice were purchased from SLC Japan (Shizuoka, Japan). Six-week-old mice were subcutaneously (s.c.)

***Correspondence to:** Investigative Treatment Division, Research Center for Innovative Oncology, National Cancer Center Hospital East, 6-5-1 Kashiwanoha, Kashiwa, Chiba 277-8577, Japan. Fax: +81-4-7134-6866. E-mail: yhmatsum@east.ncc.go.jp
Received 2 September 2007; Accepted after revision 20 November 2007
DOI 10.1002/ijc.23381
Published online 14 January 2008 in Wiley InterScience (www.interscience.wiley.com).

inoculated with 1×10^6 cells of HT-29 or HCT-116 cell line in the flank region. The length (a) and width (b) of the tumor masses were measured twice a week, and the tumor volume (TV) was calculated as follows: $TV = (a \times b^2)/2$. All animal procedures were performed in compliance with the Guidelines for the Care and Use of Experimental Animals established by the Committee for Animal Experimentation of the National Cancer Center; these guidelines meet the ethical standards required by law and also comply with the guidelines for the use of experimental animals in Japan.

Drugs

The SN-38-incorporating polymeric micelles, NK012, and SN-38 were prepared by Nippon Kayaku (Tokyo, Japan).[12] CPT-11 was purchased from Yakult Honsha (Tokyo, Japan). 5FU was purchased from Kyowa Hakko (Tokyo, Japan).

Cell growth inhibition assay

HT-29 cells were seeded in 96-well plates at a density of 2,000 cells/well in a final volume of 90 μL. Twenty-four hours after seeding, a graded concentration of NK012 or SN-38 was added concurrently with 5FU to the culture medium of the HT-29 cells in a final volume of 100 μL for drug interaction studies. The culture was maintained in the CO_2 incubator for an additional 72 hr. Then, cell growth inhibition was measured by the tetrazolium salt-based proliferation assay (WST assay; Wako Chemicals, Osaka, Japan). WST-1 labeling solution (10 μL) was added to each well and the plates were incubated at 37°C for 3 hr. The absorbance of the formazan product formed was detected at 450 nm in a 96-well spectrophotometric plate reader. Cell viability was measured and compared to that of the control cells. Each experiment was carried out in triplicate and was repeated at least 3 times. Data were averaged and normalized against the nontreated controls to generate dose-response curves.

Drug interaction analysis

The nature of interaction between NK012 or SN-38 and 5FU against HT-29 cells was evaluated by median-effect plot analyses and the combination index (CI) method of Chou and Talalay.[13] Data analysis was performed using the Calcusyn software (Biosoft, NY, USA). NK012 or SN-38 was combined with 5FU at a fixed ratio that spanned the individual IC_{50} values of each drug. The IC_{50} values were determined on the basis of the dose-response curves using the WST assay. For any given drug combination, the CI is known to represent the degree of synergy, additivity or antagonism. It is expressed in terms of fraction-affected (Fa) values, which represents the percentage of cells killed or inhibited by the drug. Isobologram equations and Fa/CI plots were constructed by computer analysis of the data generated from the median effect analysis. Each experiment was performed in triplicate with 6 gradations and was repeated at least 3 times. The resultant dose-response curves were averaged, to create a single composite dose-response curve for each combination.

In vivo analysis of the effects of NK012 combined with 5FU as compared to those of CPT-11 combined with 5FU

When the mean tumor volumes reached ~93 mm^3, the mice were randomly divided into test groups consisting of 5 mice per group (Day 0). The drugs were administered i.v. *via* the tail vein of the mice. In the groups administered NK012 or 5FU as single agents, the drug was administered on Days 0, 7 and 14. In the combined treatment groups, NK012 or CPT-11 was administered 24 hr before 5FU on Days 0, 7 and 14, according to the previously reported combination schedule for CPT-11 and 5FU.[14] Complete response (CR) was defined as tumor not detectable by palpation at 90 days after the start of treatment, at which time-point the mice were sacrificed. Tumor volume and body weight were measured twice a week. As a general rule, animals in which the tumor volume exceeded 2,000 mm^3 were also sacrificed.

Experiment 1. Evaluation of the effects of NK012 combined with 5FU and determination of the maximum tolerated dose (MTD) of NK012/5FU. By comparing the data between NK012 administered as a single agent and NK012/5FU, we evaluated the effects of the combined regimen against the s.c HT-29 tumors. A preliminary experiment showed that combined administration of NK012 15 mg/kg + 5FU 50 mg/kg every 6 days caused drug-related lethality (data not shown). To determine the MTD, therefore, we set the dosing schedule of the combined regimen at 5 or 10 mg/kg of NK012 + 50 mg/kg of 5FU three times a week.

Experiment 2. Comparison of the antitumor effect of NK012/5FU and CPT-11/5FU. Based on a comparison of the data between NK012/5FU and CPT-11/5FU against the s.c. HT-29 and HCT-116 tumors, we investigated the feasibility of the clinical application of NK012/5FU for the treatment of CRC. CPT-11/5FU was administered three times a week at the respective MTDs of the 2 drugs as previously reported, that is, CPT11 at 50 mg/kg and 5FU at 50 mg/kg, respectively.[14] NK012/5FU was administered once three times a week at the respective MTDs of the 2 drugs determined from Experiment 1.

Cell cycle analysis

Samples from the HT-29 tumors that had grown to 80–100 mm^3 were removed from the mice at 6, 24, 48, 72 and 96 hr after the administration of NK012 alone at 10 mg/kg or CPT-11 alone at 50 mg/kg. The samples were excised, minced in PBS and fixed in 70% ethanol at −20°C for 48 hr. They were then digested with 0.04% pepsin (Sigma chemical Co., St Lous, MO) in 0.1 N HCL for 60 min at 37°C in a shaking bath to prepare single-nuclei suspensions. The nuclei were then centrifuged, washed twice with PBS and stained with 40 μg/mL of propidium iodide (Molecular Probes, OR) in the presence of 100 μg/mL RNase in 1 mL PBS for 30 min at 37°C. The stained nuclei were analyzed with B-D FACSCalibur (BD Biosciences, San Jose, CA), and the cell cycle distribution was analyzed using the Modfit program (Verity Software House Topsham, ME).

Statistical analyses

Data were expressed as mean ± SD. Data were analysed with Student's t test when the groups showed equal variances (F test), or Welch's test when they showed unequal variances (F test). $p < 0.05$ was regarded as statistically significant. All statistical tests were 2-sided.

Results

Antiproliferative effects of NK012 or SN-38 administered in combination with 5FU

Figure 1*a* shows the dose-response curves for NK012 alone, 5FU alone and a combination of the two. The IC_{50} levels of NK012 and 5FU against the HT-29 cells were 39 nM and 1 μM, respectively, and the IC_{50} level of SN-38 was 14 nM (data not shown). Based on these data, the molar ratio of NK012 or SN-38:5FU of 1:1,000 was used for the drug combination studies.

Figures 1*b* and 1*c* show the median-effect and the combination index plots. Combination indices (CIs) of <1.0 are indicative of synergistic interactions between 2 agents; additive interactions are indicated by CIs of 1.0, and antagonism by CIs of >1.0. Figure 1*c* shows the combination index for NK012 and 5FU, when 2 drugs are supposed to be mutually exclusive. Marked synergism was observed between Fa 0.2 and 0.6. Theoretically, the CI method is the most reliable around an Fa of 0.5, suggesting synergistic effects of the combination of NK012 and 5FU. This synergistic effect was more evident than that of SN-38/5FU (Fig. 1*d*).

In vivo *effect of combined NK012 and 5FU*

Experiment 1. Dose optimization and effect of combined NK012 and 5FU against HT-29 tumors. Comparison of the relative tumor volumes on Day 40 revealed significant differences between

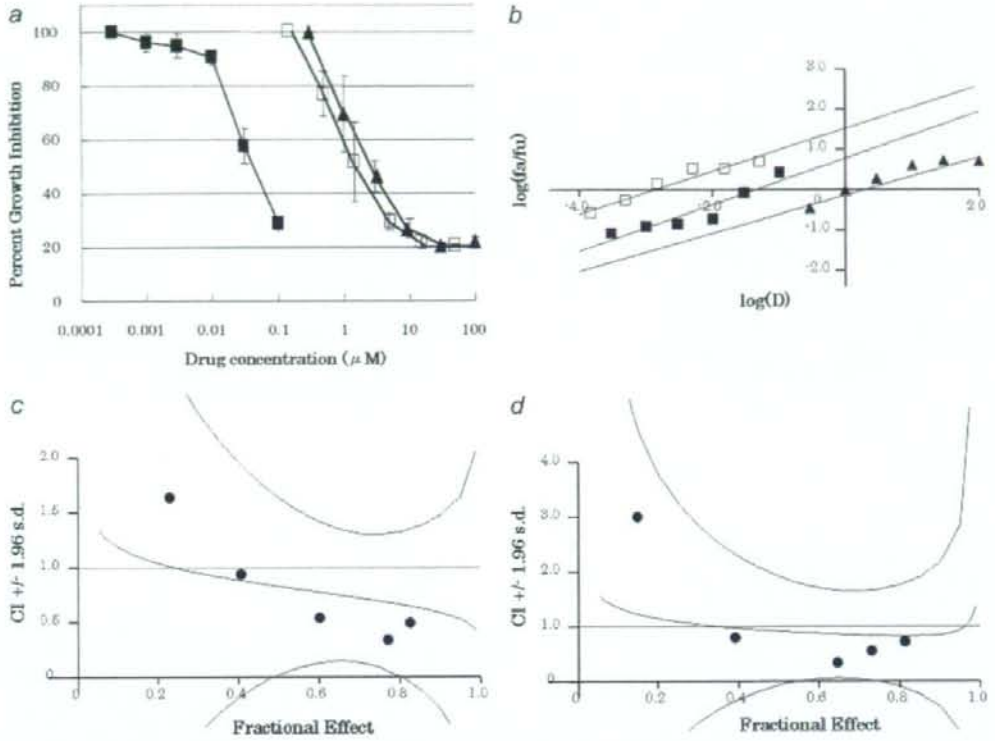

FIGURE 1 – Interaction of NK012 and 5FU *in vitro*. (*a*) Dose-response curves for NK012 alone (■), 5FU alone (▲) and their combination (□) against HT-29 cells. HT-29 cells were seeded at 2,000 cells/well. Twenty-four hours after seeding, a graded concentration of NK012 or 5FU was added to the culture medium of the HT-29 cells. Cell growth inhibition was measured by WST assay after 72 hr of treatment. Cell viability was measured and compared with that of the control cells. Each experiment was carried out independently and repeated at least 3 times. Points, mean of tripricates; bars, SD. (*b*) Median effect plot for the interaction of NK012 and 5FU. (*c*, *d*) Combination index for the interaction as a function of the level of effect (fraction effect = 0.5 is the IC_{50}). The straight line across the CI value of 1.0 indicates additive effect and CIs above and below indicate antagonism and synergism, respectively. The molar ratio of NK012/5FU (*c*) or SN-38/5FU (*d*) at 1:1,000 was tested by CI analysis. Black circles represent the CIs of the actual data points, solid lines represent the computer-derived CIs at effect levels ranging from 10 to 100% inhibition of cell growth, and the dotted lines represent the 95% confidence intervals.

those in the mice administered NK012 alone and those administered NK012/5FU at 5 mg/kg of NK012 ($p = 0.018$) (Fig. 2*a*). Although there was no statistically significant difference in the relative tumor volume measured on Day 54 between the mice administered NK012 alone and NK012/5FU at 10 mg/kg of NK012 ($p = 0.3050$), a trend of superior antitumor effect was demonstrated in the group treated with NK012/5FU at 10 mg/kg of NK012 (Fig. 2*a*). The CR rates were 20, 40 and 60% for 5 mg/kg NK012 + 50 mg/kg 5FU, 10 mg/kg NK012 alone and 10 mg/kg NK012 + 50 mg/kg 5FU, respectively. The schedule of 10 mg/kg NK012 + 50 mg/kg 5FU resulted in no remarkable toxicity in terms of body weight changes, and these doses were determined as representing the MTDs (Fig. 2*b*).

Experiment 2. Comparison of the antitumor effect of combined NK012/5FU and CPT-11/5FU against HT-29 and HCT-116 tumors. The therapeutic effect of NK012/5FU on Day 60 was significantly superior to that of CPT-11/5FU against the HT-29 tumors ($p = 0.0004$) (Fig. 3*a*). A more potent antitumor effect, namely, a 100% CR rate, was obtained in the NK012/5FU group as compared to the 0% CR rate in the CPT-11/5FU group. Although no statistically significant difference in the relative tumor volume on Day 61 was demonstrated between the NK012/5FU and CPT-11/5FU in the case of the HCT-116 tumors ($p = 0.2230$), a trend of superior antitumor effect against these tumors was observed in the NK012/5FU treatment group (Fig. 3*b*). The CR rates for the case of the HCT-116 tumors were 0% in both NK012/5FU and CPT-11/5FU groups.

Specificity of cell cycle perturbation

We studied the differences in the effects between NK012 10 mg/kg and CPT-11 50 mg/kg on the cell cycle (Fig. 4*a*). The data indicated that both NK012 and CPT-11 tended to cause accumulation of cells in the S phase, although the effect of NK012 was stronger and maintained for a more prolonged period than that of CPT-11; the maximal percentage of S-phase cells in the total cell population in the tumors was 34% at 24 hr after the administration of CPT-11, whereas it was 39% at 48 hr after the administration of NK012 (Figs. 4*b*, and 4*c*).

Discussion

Our primary endpoint was to clarify the advantages of NK012 over CPT-11 administered in combination with 5FU. We demonstrated that combined NK012 and 5FU chemotherapy exerts more

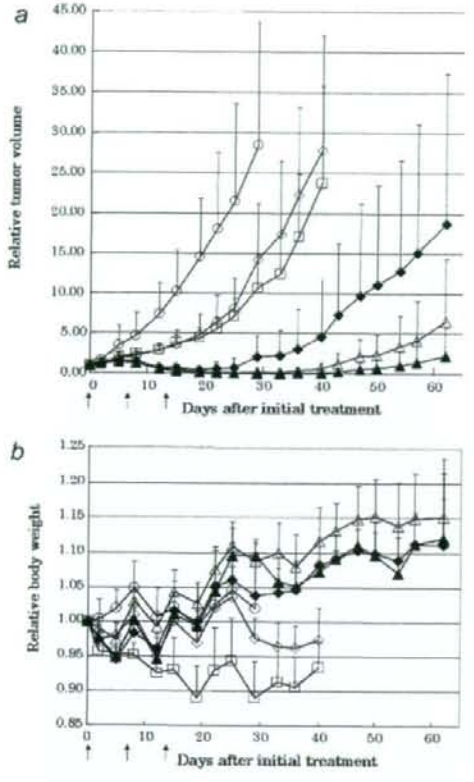

FIGURE 2 – Effect of NK012 alone or NK012 in combination with 5FU against HT-29 tumor-bearing mice. Points, mean; bars, SD. (*a*) Antitumor effect of each regimen on Days 0, 7 and 14. (○) control, (□) 5FU 50 mg/kg alone, (◇) NK012 5 mg/kg alone, (◆) NK012 5 mg/kg 24 hr before 5FU 50 mg/kg, (△) NK012 10 mg/kg alone, (▲) NK012 10 mg/kg 24 hr before 5FU 50 mg/kg. (*b*) Changes in the relative body weight. Data were derived from the same mice as those used in the present study.

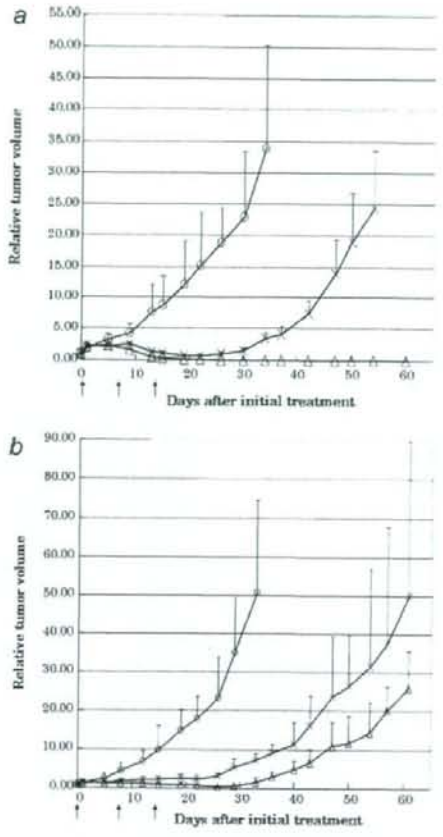

FIGURE 3 – Effect of NK012/5FU as compared with that of CPT11/5FU against HT-29 (*a*) or HCT-116 (*b*) tumor-bearing mice. Antitumor effect of each schedule on Days 0, 7 and 14. (○) control, (×) CPT-11 50 mg/kg 24 hr before 5FU 50 mg/kg, (△) NK012 10 mg/kg 24 hr before 5FU 50 mg/kg. Points, mean; bars, SD.

synergistic activity *in vitro* and significantly greater antitumor activity against human CRC xenografts as compared to CPT-11/5FU. The combination of NK012 and 5FU is considered to hold promise of clinical benefit for patients with CRC.

CPT-11, a topoisomerase-I inhibitor, and 5FU, a thymidilate synthase inhibitor, have been demonstrated to be effective agents for the treatment of CRC. A combination of these 2 drugs has also been demonstrated to be clearly more effective than either CPT-11 or 5FU/LV administered alone *in vivo* and in clinical settings.[1,2,14] Administration of 5FU by infusion with CPT-11 was shown to be associated with reduced toxicity and an apparent improvement in survival as compared to that of administration of the drug by bolus injection with CPT-11.[1,2] This synergistic enhancement may result from the mechanism of action of the 2 drugs; CPT-11 has been reported to cause accumulation of cells in the S phase, and 5FU infusion is known to cause DNA damage specifically in cells of the S phase.[14] On the basis of this background, our results suggesting the more pronounced and more prolonged accumulation of the tumor cells in the S phase caused by NK012 as compared with that by CPT-11 may explain the more effective synergy of the former administered with 5FU infusion. This may be attributable to accumulation of NK012 due to the enhanced permeability and retention (EPR) effect.[9] It is also speculated that NK012 allows sustained release of free SN-38, which may move more freely in the tumor interstitium.[15] Otherwise NK012 itself could internalize into cells to localize in several cytoplasmic organelles as reported by Savic *et al.*[16] These characteristics of NK012 may be responsible for its more potent antitumor activity observed in this study, because CPT-11 has been reported to show time-dependent growth-inhibitory activity against the tumor cells.[17]

The major dose-limiting toxicities of CPT-11 are diarrhea and neutropenia. SN-38, the active metabolite of CPT-11, may cause CPT-11-related diarrhea as a result of mitotic -inhibitory activity.[18] Because it undergoes significant biliary excretion, SN-38 may have a potentially long residence time in the gastrointestinal tract that may be associated with prolonged diarrhea.[19,20] In our previous report, we evaluated the tissue distribution of SN-38 after administration of an equimolar amount of NK012 (20 mg/kg) and CPT-11 (30 mg/kg), and found no difference in the level of SN-38 accumulation in the small intestine.[12] A significant antitumor effect of NK012 with a lower incidence of diarrhea was also dem-

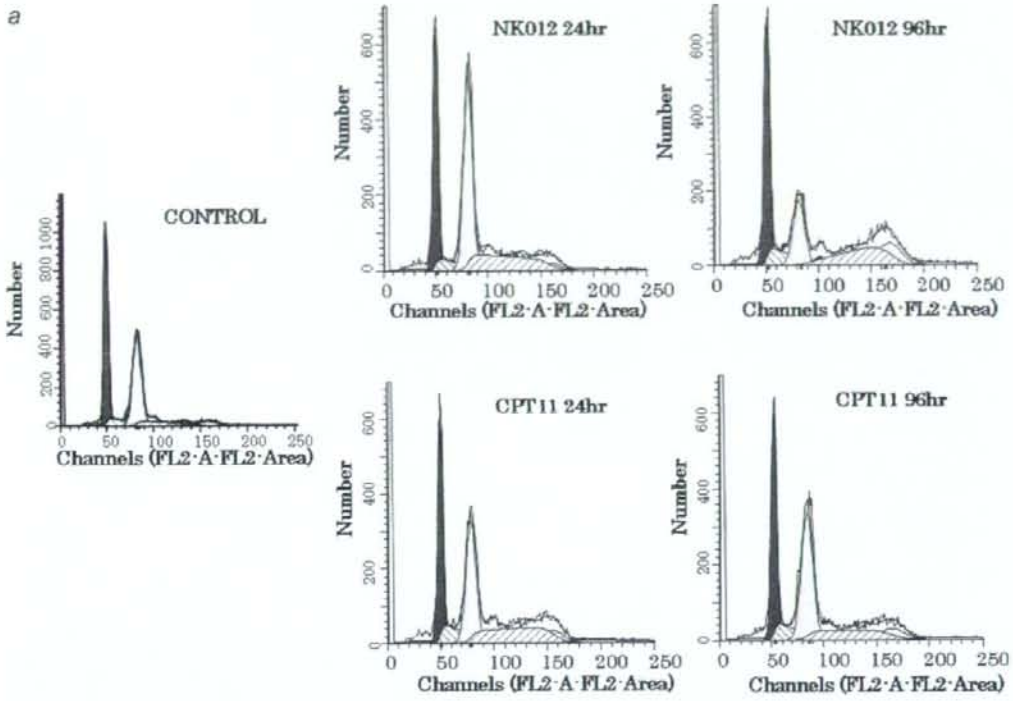

FIGURE 4 – Cell cycle analysis of HT-29 tumor cells collected 24, 48, 72 and 96 hr after administration of NK012 at 10 mg/kg alone or CPT-11 at 50 mg/kg alone using the Modfit program (Verity Software House Topsham, ME). (*a*) Cell cycle analysis of HT-29 tumor cells 24 and 96 hr after administration of NK012 at 10 mg/kg or CPT-11 at 50 mg/kg, respectively. (*b*) Cell cycle distribution of tumor cells 0, 24, 48, 72 and 96 hr after treatment with NK012 at 10 mg/kg. (*c*) Cell cycle distribution of tumor cells 0, 24, 48, 72 and 96 hr after treatment with CPT-11 at 50 mg/kg.

onstrated as compared to that observed with CPT-11 in a rat mammary tumor model.[21] Combined administration of CPT-11 with 5FU/LV infusion appears to be associated with acceptable toxicity in patients with CRC. In addition, no significant difference in the frequency of Grade 3/4 diarrhea was noted between patients treated with FOLFIRI (CPT-11 regimen with bolus and infusional 5FU/LV) and those treated with FOLFOX6 (oxaliplatin regimen with bolus and infusional 5FU/LV).[22,23] Our *in vivo* data actually revealed no severe body weight loss in the NK012/5FU group. Consequently, we expect that the NK012/5FU regimen, especially

with infusional 5FU, may be an attractive arm for a Phase III trial in CRC, with CPT-11/5FU as the control arm. We have already initiated a Phase I trial of NK012 in patients with advanced solid tumors based on the data suggesting higher efficacy and lower toxicity of this preparation than CPT-11 *in vivo*.[12]

In conclusion, we demonstrated that combined NK012 and 5FU chemotherapy exerts significantly greater antitumor activity against human CRC xenografts as compared to CPT-11/5FU, indicating the necessity of clinical evaluation of this combined regimen.

References

1. Saltz LB, Douillard JY, Pirotta N, Alakl M, Gruia G, Awad L, Elfring GL, Locker PK, Miller LL. Irinotecan plus fluorouracil/leucovorin for metastatic colorectal cancer: a new survival standard. Oncologist 2001;6:81–91.
2. Douillard JY, Cunningham D, Roth AD, Navarro M, James RD, Karasek P, Jandik P, Iveson T, Carmichael J, Alakl M, Gruia G, Awad L, et al. Irinotecan combined with fluorouracil compared with fluorouracil alone as first-line treatment for metastatic colorectal cancer: a multicentre randomised trial. Lancet 2000;355:1041–7.
3. Takimoto CH, Arbuck SG. Topoisomerase I targeting agents: the camptothecins. In: Chabner BA, Lango DL, eds. Cancer chemotherapy and biotherapy: principal and practice, 3rd ed. Philadelphia, PA: Lippincott Williams and Wilkins, 2001. 579–646.
4. Slatter JG, Schaaf LJ, Sams JP, Feenstra KL, Johnson MG, Bombardt PA, Cathcart KS, Verburg MT, Pearson LK, Compton LD, Miller LL, Baker DS, et al. Pharmacokinetics, metabolism, and excretion of irinotecan (CPT-11) following I.V. infusion of [(14)C]CPT-11 in cancer patients. Drug Metab Dispos 2000;28:423–33.
5. Rothenberg ML, Kuhn JG, Burris HA, III, Nelson J, Eckardt JR, Tristan-Morales M, Hilsenbeck SG, Weiss GR, Smith LS, Rodriguez GI, Rock MK, Von Hoff DD. Phase I and pharmacokinetic trial of weekly CPT-11. J Clin Oncol 1993;11:2194–204.
6. Guichard S, Terret C, Hennebelle I, Lochon I, Chevreau P, Fretigny E, Selves J, Chatelut E, Bugat R, Canal P. CPT-11 converting carboxylesterase and topoisomerase activities in tumour and normal colon and liver tissues. Br J Cancer 1999;80:364–70.
7. Gradishar WJ, Tjulandin S, Davidson N, Shaw H, Desai N, Bhar P, Hawkins M, O'Shaughnessy J. Phase III trial of nanoparticle albumin-bound paclitaxel compared with polyethylated castor oil-based paclitaxel in women with breast cancer. J Clin Oncol 2005;23:7794–803.
8. Muggia FM. Liposomal encapsulated anthracyclines: new therapeutic horizons. Curr Oncol Rep 2001;3:156–62.
9. Matsumura Y, Maeda H. A new concept for macromolecular therapeutics in cancer chemotherapy: mechanism of tumoritropic accumulation of proteins and the antitumor agent smancs. Cancer Res 1986;46:6387–92.
10. Zhang JA, Xuan T, Parmar M, Ma L, Ugwu S, Ali S, Ahmad I. Development and characterization of a novel liposome-based formulation of SN-38. Int J Pharm 2004;270:93–107.
11. Kraut EH, Fishman MN, LoRusso PM, Gorden MS, Rubin EH, Haas A, Fetterly GJ, Cullinan P, Dul JL, Steinberg JL. Final result of a phase I study of liposome encapsulated SN-38 (LE-SN38): safety, pharmacogenomics, pharmacokinetics, and tumor response [abstract 2017]. Proc Am Soc Clin Oncol 2005;23:139S.
12. Koizumi F, Kitagawa M, Negishi T, Onda T, Matsumoto S, Hamaguchi T, Matsumura Y. Novel SN-38-incorporating polymeric micelles, NK012, eradicate vascular endothelial growth factor-secreting bulky tumors. Cancer Res 2006;66:10048–56.
13. Chou TC, Talalay P. Quantitative analysis of dose-effect relationships: the combined effects of multiple drugs or enzyme inhibitors. Adv Enzyme Regul 1984;22:27–55.
14. Azrak RG, Cao S, Slocum HK, Toth K, Durrani FA, Yin MB, Pendyala L, Zhang W, McLeod HL, Rustum YM. Therapeutic synergy between irinotecan and 5-fluorouracil against human tumor xenografts. Clin Cancer Res 2004;10:1121–9.
15. Jain RK. Barriers to drug delivery in solid tumors. Sci Am 1994; 271:58–65.
16. Savic R, Luo L, Eisenberg A, Maysinger D. Micellar nanocontainers distribute to defined cytoplasmic organelles. Science 2003;300:615–18.
17. Kawato Y, Aonuma M, Hirota Y, Kuga H, Sato K. Intracellular roles of SN-38, a metabolite of the camptothecin derivative CPT-11, in the antitumor effect of CPT-11. Cancer Res 1991;51:4187–91.
18. Slater R, Radstone D, Matthews L, McDaid J, Majeed A. Hepatic resection for colorectal liver metastasis after downstaging with irinotecan improves survival. Proc Am Soc Clin Oncol 2003;22(abstract 1287).
19. Araki E, Ishikawa M, Iigo M, Koide T, Itabashi M, Hoshi A. Relationship between development of diarrhea and the concentration of SN-38, an active metabolite of CPT-11, in the intestine and the blood plasma of athymic mice following intraperitoneal administration of CPT-11. Jpn J Cancer Res 1993;84:697–702.
20. Atsumi R, Suzuki W, Hakusui H. Identification of the metabolites of irinotecan, a new derivative of camptothecin, in rat bile and its biliary excretion. Xenobiotica 1991;21:1159–69.
21. Onda T, Nakamura I, Seno C, Matsumoto S, Kitagawa M, Okamoto K, Nishikawa K, Suzuki M. Superior antitumor activity of NK012, 7-ethyl-10-hydroxycamptoyhecin-incorporating micellar nanoparticle, to irrinotecan. Proc Am Assoc Cancer Res 2006;47:720s(abstract 3062).
22. Tournigand C, Andre T, Achille E, Lledo G, Flesh M, Mery-Mignard D, Quinaux E, Couteau C, Buyse M, Ganem G, Landi B, Colin P, et al. FOLFIRI followed by FOLFOX6 or the reverse sequence in advanced colorectal cancer: a randomized GERCOR study. J Clin Oncol 2004;22:229–37.
23. Colucci G, Gebbia V, Paoletti G, Giuliani F, Caruso M, Gebbia N, Carteni G, Agostara B, Pezzella G, Manzione L, Borsellino N, Misino A, et al. Phase III randomized trial of FOLFIRI versus FOLFOX4 in the treatment of advanced colorectal cancer: a multicenter study of the Gruppo Oncologico Dell'Italia Meridionale. J Clin Oncol 2005; 23:4866–75.

Overexpression of Class III β-Tubulin Predicts Good Response to Taxane-Based Chemotherapy in Ovarian Clear Cell Adenocarcinoma

Daisuke Aoki,[1] Yoshinao Oda,[3] Satoshi Hattori,[8] Ken-ichi Taguchi,[7] Yoshihiro Ohishi,[3] Yuji Basaki,[5,6] Shinji Oie,[2] Nao Suzuki,[10] Suminori Kono,[4] Masazumi Tsuneyoshi,[3] Mayumi Ono,[5,6] Takashi Yanagawa,[8] and Michihiko Kuwano[6,9]

Abstract

Purpose: Of the various microtubule-associated molecules, β-tubulin III has been reported to be closely associated with the therapeutic efficacy of taxane-based chemotherapy against ovarian cancer. Stathmin and microtubule-associated protein 4 (MAP4) have been reported to play an important role in microtubule stabilization. In this study, we investigated whether expression of these microtubule-associated factors affects the therapeutic efficacy of taxane-based chemotherapy in ovarian clear cell adenocarcinoma.

Experimental Design: Drug sensitivity of paclitaxel or cisplatin was assessed in ovarian cancer cell lines treated with small interfering RNA of tubulin isoforms, MAP4, and stathmin. We examined 94 surgically resected ovarian clear cell adenocarcinoma specimens from patients treated with taxane-containing regimens ($n = 44$) and with taxane-free regimens ($n = 50$), using immunohistochemistry to detect expression of β-tubulin III, stathmin, and MAP4.

Results: Knockdown of β-tubulin III and IV specifically conferred drug resistance to paclitaxel in one ovarian cancer cell line, but not to other molecules. Estimated overall survival revealed a significant synergistic effect between taxane and β-tubulin III in patients with ovarian clear cell adenocarcinoma. Of three microtubule-related molecules, among the taxane-based chemotherapy group, cases with higher β-tubulin III expression were associated with a significantly more favorable prognosis compared with those having lower β-tubulin III expression. By contrast, there was no statistical significance in the synergistic relationships between stathmin and taxane or between MAP4 and taxane.

Conclusions: Taxane-based chemotherapy was effective for patients with ovarian clear cell adenocarcinomas who were positive for β-tubulin III but not for those who were negative for these proteins.

Microtubules are the principal target of a large and diverse group of natural-product anticancer therapeutic drugs, particularly of two major classes of antimicrotubule agents: the vinca alkaloids and the taxanes (1). Microtubules are composed of polymers of heterodimers that consist of two closely related polypeptides, α-tubulin and β-tubulin, which in turn contain α- or β-subunits and at least six isotypes encoded by different genes. Isotype composition influences the intrinsic dynamics of microtubules, and the sensitivity of microtubules to depolymerizing and polymerizing agents is related to the composition of tubulin isotypes or microtubule-associated proteins (MAP; ref. 2). MAPs, important components of the tubulin and microtubule system, can bind to the microtubule wall and stabilize microtubules (3). MAP2 and MAP-τ are abundantly expressed in mature neurons, and MAP4 is ubiquitously expressed in both proliferating and differentiated cells (4). Stathmin is also the founding member of the microtubule-destabilizing family of proteins, which regulate the dynamics of microtubule polymerization and depolymerization. Stathmin is expressed at high levels in a variety of human cancers

Authors' Affiliations: [1]Department of Obstetrics and Gynecology, School of Medicine, Keio University, and [2]Personalized Medicine Research Laboratory, Taiho Pharmaceutical Co Ltd., Tokyo, Japan; Departments of [3]Anatomic Pathology and [4]Preventive Medicine, Graduate School of Medical Sciences, [5]Department of Pharmaceutical Oncology, Graduate School of Pharmaceutical Sciences, and [6]Innovation Center for Medical Redox Navigation, Kyushu University, and [7]Kyushu National Cancer Center, Fukuoka, Japan; [8]Biostatistics Center and [9]Research Center for Innovative Cancer Therapy, Kurume University, Kurume City, Japan; and [10]Department of Obstetrics and Gynecology, School of Medicine, Saint. Marianna University, Kawasaki, Japan

Received 8/16/08; revised 10/31/08; accepted 11/7/08.

Grant support: Grant-in-Aid for Scientific Research on Priority Areas, Cancer, from the Ministry of Education, Culture, Sports, Science and Technology of Japan (M. Ono), and by the Third Term Comprehensive Control Research for Cancer from the Ministry of Health, Labor and Welfare, Japan (M. Kuwano). This study was also supported, in part, by the Formation of Innovation Center for Fusion of Advanced Technologies, Kyushu University, Japan (M. Ono, Y. Basaki, and M. Kuwano).

The costs of publication of this article were defrayed in part by the payment of page charges. This article must therefore be hereby marked *advertisement* in accordance with 18 U.S.C. Section 1734 solely to indicate this fact.

Note: Supplementary data for this article are available at Clinical Cancer Research Online (http://clincancerres.aacrjournals.org/).

D. Aoki, Y. Oda, S. Hattori, K. Taguchi, Y. Ohishi, and Y. Basaki contributed equally to this work.

Requests for reprints: Daisuke Aoki, Department of Obstetrics and Gynecology, School of Medicine, Keio University, 35 Shinanomachi, Shinjuku-ku, Tokyo 160-8582, Japan. Phone: 81-3-3353-1211; Fax: 81-3-3226-1667; E-mail: aoki@sc.itc.keio.ac.jp.

doi:10.1158/1078-0432.CCR-08-1274

Translational Relevance

It has been reported that β-tubulin III, one of microtubule-associated molecules, was expected to be a useful biomarker for the clinical efficacy of taxane-based chemotherapy against human ovarian cancer. These studies have been conducted in serous adenocarcinoma of ovarian cancer. Previous reports show, however, that ovarian clear cell adenocarcinoma constituted about 20% of ovarian adenocarcinoma in Japan, although only 2% to 5% of cases of ovarian cancer worldwide were clear cell adenocarcinoma. Clear cell adenocarcinoma, which is a rare variant in western counties, has been recognized as a chemoresistant phenotype compared with serous adenocarcinoma, which is the most widespread ovarian cancer. This study aimed to identify a predictive marker for the clinical efficacy of taxane-based chemotherapy against ovarian clear cell adenocarcinoma. In this study, we found that a taxane-based regimen was effective for patients with ovarian clear cell adenocarcinomas who were positive for stathmin or β-tubulin III.

and also plays a role in altered drug sensitivity in human cancer cells, including ovarian cancer cells (5, 6).

The antitumor drug taxane stabilizes microtubules and reduces their dynamics, promoting mitotic arrest and cell death. Paclitaxel, a representative anticancer agent of the taxanes, was initially defined by Horowitz and colleagues, and its binding sites are distinct from those of colchicine, podophyllotoxin, and the vinca alkaloids (7, 8). Paclitaxel initially received regulatory approval for the treatment of patients with ovarian cancer after failure of first-line or subsequent chemotherapy (9). In a Gynecologic Oncology Group study (GOG-111), it was thus determined to be the primary induction therapy in suboptimally debulked stage III and IV ovarian cancer, which mainly consists of serous adenocarcinoma (10). This study first compared the therapeutic efficacy of paclitaxel/cisplatin and cyclophosphamide/cisplatin in patients with ovarian cancer (10). The paclitaxel arm showed a distinct advantage in terms of progression-free survival (PFS) as well as overall survival (OS). A clinical trial by the European Organization for Research and Treatment of Cancer and the National Cancer Institute of Canada also showed that a paclitaxel/cisplatin regimen improved both PFS and OS (11). Another clinical trial study, however, reported that survival in the paclitaxel arm was similar to that seen in the control arm that received either carboplatin or cisplatin, doxorubicin, and cyclophosphamide (12). It remains unclear whether paclitaxel-cisplatin (or carboplatin) therapy is superior to cyclophosphamide/cisplatin (or carboplatin) therapy.

Of the various molecular markers related to drug sensitivity to taxanes, class III β-tubulin is expected to be a useful biomarker for the clinical efficacy of paclitaxel-based chemotherapy. Class III β-tubulin is hypothesized to counteract suppression of microtubule dynamics (13). Ferlini et al. reported that a novel taxane targeting class III β-tubulin overcame paclitaxel resistance, suggesting close involvement of this tubulin isotype in drug sensitivity to paclitaxel (14). Mozzetti et al. reported that class III β-tubulin overexpression represented a prominent mechanism of resistance to paclitaxel-platinum treatment in ovarian cancer (15). Moreover, class III β-tubulin overexpression could be useful in identifying poor clinical outcome in patients with advanced ovarian cancer who are treated with platinum/paclitaxel, those mainly affected with serous adenocarcinoma (16). These studies have been conducted mainly in serous adenocarcinoma of ovarian cancer. It remains unknown, however, whether class III β-tubulin overexpression is also predictive of poor outcome in clear cell adenocarcinoma, which is a rare variant in western countries, where it is reported to constitute 5% to 10% of ovarian carcinomas (17–19). Clear cell adenocarcinoma has been recognized as a chemoresistant phenotype (20, 21).

Japanese investigators have reported that clear cell adenocarcinoma constitutes about 20% of ovarian carcinomas in Japan (20, 22), although clear cell adenocarcinoma of the ovary accounts for only 2% to 5% of cases enrolled in large-scale randomized trials worldwide (22, 23). Thus, it is unclear whether carboplatin/paclitaxel therapy, which was introduced broadly as a standard regimen for epithelial ovarian cancer based on the results of such trials, can be readily applied for clear cell adenocarcinoma. Development of novel treatment strategies based on molecular biological characteristics is further required for clear cell adenocarcinoma.

In the present study, we addressed whether expression of β-tubulin III, MAP4, and stathmin could affect the efficacy of taxane-based therapeutic regimens against clear cell adenocarcinoma. Using immunohistochemical analysis of surgically resected clinical samples of clear cell adenocarcinoma, we examined expression levels of the above three biomarkers. In comparison with ovarian cancer patients treated with taxane-free regimens, we observed a significant and specific association of β-tubulin III expression with therapeutic outcomes of ovarian cancer treated with taxane-based regimens. We discuss whether the expression of β-tubulin III could be a predictive marker for the clinical efficacy of taxane-based chemotherapy against ovarian clear cell adenocarcinoma.

Materials and Methods

Cells and reagents. The human ovarian cell lines OVCAR-3 and SKOV-3, which expressed β-tubulins (I, II, III, and IV), MAP4, and stathmin, were obtained from the American Type Culture Collection. Cells were grown in Ham's F-12 Medium (Nissui Seiyaku Co.) with 10% fetal bovine serum (FetalClone III; Hyclone), 100 IU/mL penicillin, and 100 μg/mL streptomycin (Life Technologies, Inc.) in a humidified atmosphere of 5% CO_2 at 37°C. Paclitaxel (Taxol injection) and cisplatin (Briplatin injection) purchased from Bristol-Myers Squibb were clinically used. The polyclonal antistathmin was obtained from Calbiochem. The monoclonal class III β-tubulin antibody (clone 5G8) was obtained from Promega. The monoclonal MAP4 antibody (clone 18) was purchased from BD Transduction Laboratories.

Silencing of β-tubulins (I, II, III, IV), MAP4, and stathmin genes. To reduce the expression of some genes, we used Stealth RNAi (Invitrogen Life Technologies) to knock down the expression of β-tubulin I (NM_030773_stealth_706), β-tubulin II (NM_001069_stealth_1444), β-tubulin III (NM_006086_stealth_233), β-tubulin IV (NM_006087_stealth_352), MAP4 (NM_002375_stealth_2042), and stathmin (STMN1-HSS142799). Subconfluent human ovarian cells were cultured overnight in Opti-MEM I medium (Invitrogen Life

Technologies) without antibiotics, then 40 nmol/L small interfering RNA (siRNA) and Lipofectamine RNAiMax (Invitrogen) were applied according to the manufacturer's instructions. After 32 h, cells were detached from the culture plates and seeded into 96-well plates in F-12 medium with 10% fetal bovine serum. After a further 16-h incubation, paclitaxel or cisplatin was applied and cells were cultured for 3 d more. The numbers of cells were estimated by WST-8. The IC_{50} value was estimated from the regression line of log-logit plots of T/C (%) value versus drug concentration. The assays were carried out in quadruplicate.

Quantitative real-time PCR. RNA was reverse-transcribed from random hexamers using AMV reverse transcriptase (Promega). Real-time quantitative PCR was done using the Real-Time PCR system 7300 (Applied Biosystems). In brief, the PCR amplification reaction mixtures (20 μL) contained cDNA, primer pairs, the dual-labeled fluorogenic probe, and TaqMan Universal PCR Master Mix (Applied Biosystems). The thermal cycle conditions included maintaining the reactions at 50°C for 2 min and at 95°C for 10 min, and then alternating for 40 cycles between 95°C for 15 s and 60°C for 1 min. The primer pairs and probes were obtained from Applied Biosystems. The relative gene expression for each sample was determined using the formula $2^{(-\text{delta Ct})} = 2^{(\text{Ct (GAPDH)}-\text{Ct (target)})}$, which reflected the target gene expression normalized to GAPDH levels.

Patients. Ninety-four patients with primary ovarian clear cell adenocarcinoma, who had undergone debulking surgery at Keio University Hospital from 1983 to 2005, were examined. The histopathologic diagnoses of the all cases were confirmed according to the most recent WHO classification (WHO 2003). Patients were staged according to the International Federation of Obstetrics and Gynecology (FIGO) classification (24). Forty-four patients underwent chemotherapy using regimens containing taxanes [paclitaxel plus carboplatin (n = 39), paclitaxel plus cisplatin (n = 3), docetaxel plus cisplatin (n = 2); paclitaxel, 180 mg/m^2 body surface/day 1, docetaxel, 70 mg/m^2 body surface/day 1, cisplatin, 60 mg/m^2 body surface/day 1, and carboplatin, area under the curve 6/day 1]. Fifty patients received taxane-free regimens [CAP groups (n = 36): cisplatin (60 mg/m^2 body surface/day 1), epirubicin (50 mg/m2 body surface/day 1), and cyclophosphamide (500 mg/m^2 body surface/day 1); CAP plus fluorouracil (n = 1), CAP plus tegafur-uracil (n = 2), cisplatin plus cyclophosphamide (n = 11)]. The doses of carboplatin were calculated using Calvert's formula.

The effect of chemotherapy was evaluated approximately every 6 mo by computed tomography after 6 cycles of administration of chemotherapy. After chemotherapy, all patients were followed up every 2 mo for the first year, every 3 to 4 mo for the next 2 y, and every 6 mo

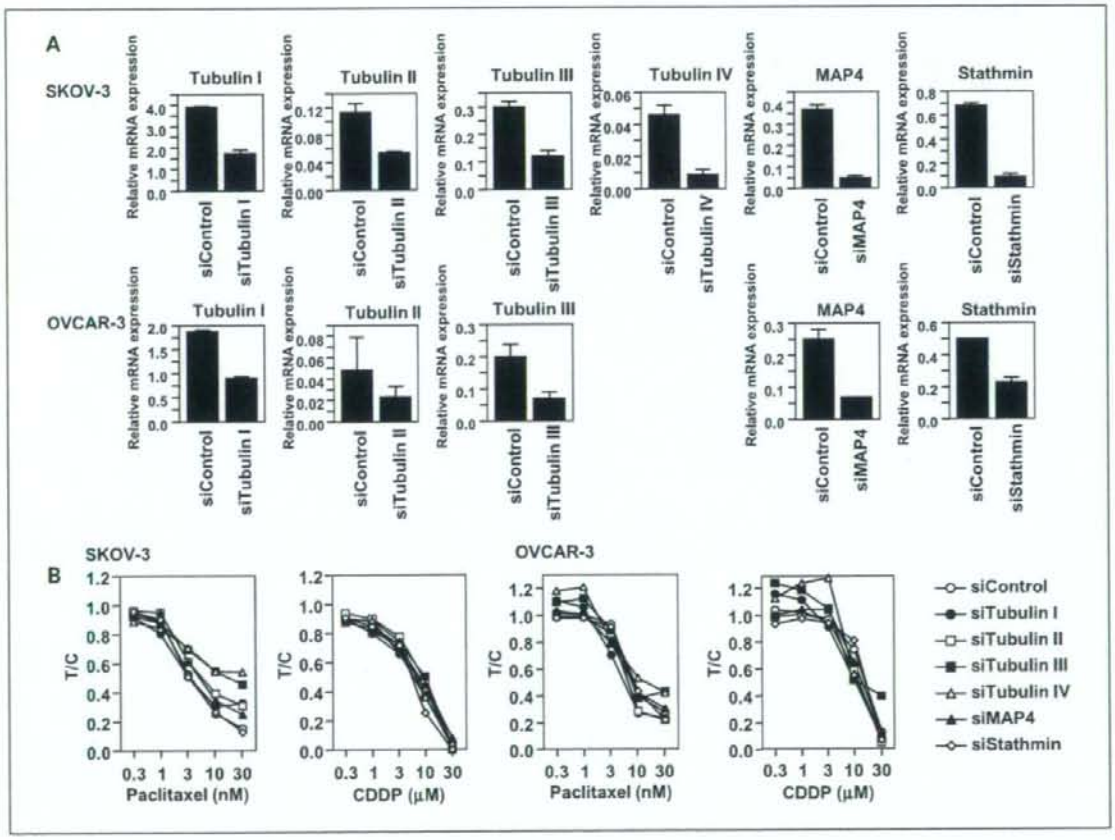

Fig. 1. Drug sensitivity to paclitaxel or cisplatin in human ovarian cancer cells treated with siRNA for β-tubulin isoforms, MAP4, and stathmin. *A*, mRNA expression of β-tubulin isoforms (I, II, III, IV), MAP4, and stathmin after treatment with respective siRNA for 48 h were determined by real-time PCR analysis. The expression of β-tubulin IV mRNA in OVCAR-3 cells was not detected. *B*, cells treated with respective siRNA were seeded into 96-well plates at 2 × 10^3 cells/0.1 mL/well and incubated overnight. On the following day, a 100-μL aliquot containing paclitaxel or cisplatin was added to the wells and cultured for a further 3 d. The number of viable cells was estimated using the WST-8 assay. The assays were carried out in quadruplicate.

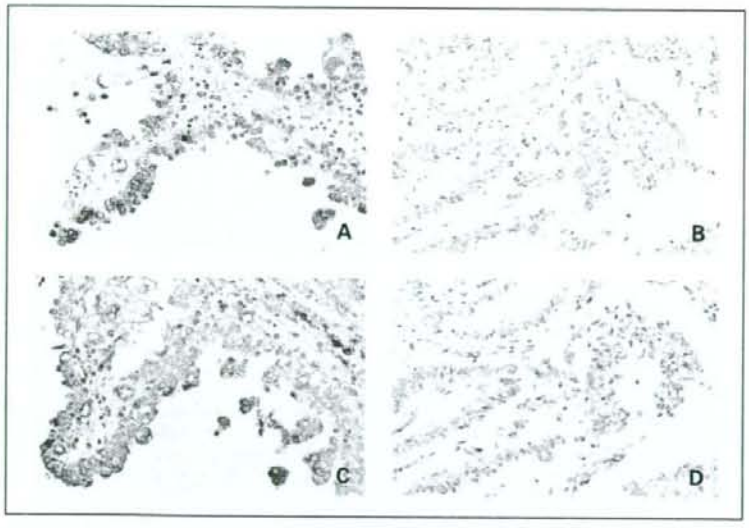

Fig. 2. *A* and *C*, stage IIc clear cell adenocarcinoma of a 55-year-old woman treated with the paclitaxel-carboplatin regimen. Cytoplasmic strong expression of stathmin (*A*, >15%) and β-tubulin III (*C*, score 7) can be diffusely observed in the tumor cells. The patient currently shows no evidence of disease 2,487 d (83 mo) after surgery. *B* and *D*, stage IIc tumor of a 56-year-old woman treated with the paclitaxel-carboplatin regimen. A few tumor cells (<15%) show only faint immunoreactivity for stathmin in the cytoplasm or nuclei, which was judged as negative (*C*). β-Tubulin III can be recognized in 10% of tumor cells with intermediate intensity and was interpreted as negative (score 4; *D*). This patient died of disease 447 d (15 mo) after initial surgery.

thereafter. Clinical outcome was measured by PFS and OS. PFS was defined as the interval from the date of first treatment (laparotomy or the first administration of neoadjuvant chemotherapy) to the date of the diagnosis of progression. We obtained informed consent from all patients, and personal information was removed from all samples before analysis.

Immunohistochemistry. Surgically resected specimens were fixed with 10% formalin and embedded in paraffin. Sections 4-μm thick on silane-coated slides were stained using the streptavidin-biotin-peroxidase method with a Histofine SAB-PO kit (Nichirei) according to the manufacturer's instructions. At least one representative section without degenerative change or necrosis was examined in each tumor. After deparaffinization, rehydration, and inhibition of endogenous peroxidase, sections were exposed to the primary antibodies at 4°C overnight. The dilutions of the primary antibody were as follows: MAP4, 1:1500; stathmin, 1:1000; and β-tubulin III, 1:200. After incubation of the secondary antibody and the streptavidin-biotin complex at room temperature, the sections were then incubated in 3 3′- diaminobenzidine, counterstained with hematoxylin, and mounted. For all antibody staining, sections were pretreated with microwave irradiation for antigen retrieval.

Immunohistochemical results were evaluated and scored by three pathologists (Y. Oda, K. Taguchi, and Y. Ohishi) without knowledge of patient clinical data. MAP4 and stathmin immunoreactivity was scored by estimating the percentage of labeled tumor cells. When >80% of the tumor cells showed immunoreactivity for MAP4, we judged the case to be positive. For stathmin expression, the cutoff value was 15%, based on a previous study (25). For class III β-tubulin expression, we evaluated the proportion and intensity of the immunoreactive cells following the protocol used to evaluate estrogen/progesterone receptors in breast cancer, proposed by Allred et al. (26, 27). Cases with a total score of ≥7 were regarded as positive.

Statistical analysis. Statistical analysis was conducted for OS and PFS to examine the effects of MAP4, stathmin, and β-tubulin III on taxane efficacy. Product-limit estimators of survival functions were obtained, respectively, relative to positivity and negativity of each marker in the patients to investigate the relationship between regimens and markers. To adjust for possible confounding factors, Cox proportional hazards models were applied. The covariates considered were a treatment indicator (0, taxane-free regimen; 1, taxane-based regimen), marker (0, negative; 1, positive), their interaction, age, two dummy variables representing FIGO stage and peritoneal cytodiagnosis (FIGO stage I-II with peritoneal cytodiagnosis negative, FIGO stage I-II with peritoneal cytodiagnosis positive, and FIGO stage III-IV) and size of residual tumor (0, <1 cm; 1, ≥1 cm).

Taking into account the size of the dataset, the latter four covariates were summarized into a propensity score (28, 29) by fitting logistic regression models with those variables to the data. The primary interest

Table 1. Correlation between positive or negative expression of MAP4, stathmin, and β-tubulin III and tumor stage or residual tumor

	FIGO stage		Residual tumor	
	I/II (n = 67)	III/IV (n = 27)	No (n = 74)	Yes (n = 20)
	No. of patients (%)	No. of patients (%)	No. of patients (%)	No. of patients (%)
MAP4 (-)	36 (54)	12 (44)	39 (53)	9 (45)
MAP4 (+)	31 (46)	15 (56)	35 (47)	11 (55)
Stathmin (-)	29 (43)	11 (41)	33 (45)	7 (35)
Stathmin (+)	38 (57)	16 (59)	41 (55)	13 (65)
β-tubulin III (-)	30 (45)	11 (41)	33 (45)	8 (40)
β-tubulin III (+)	37 (45)	16 (59)	41 (55)	12 (60)

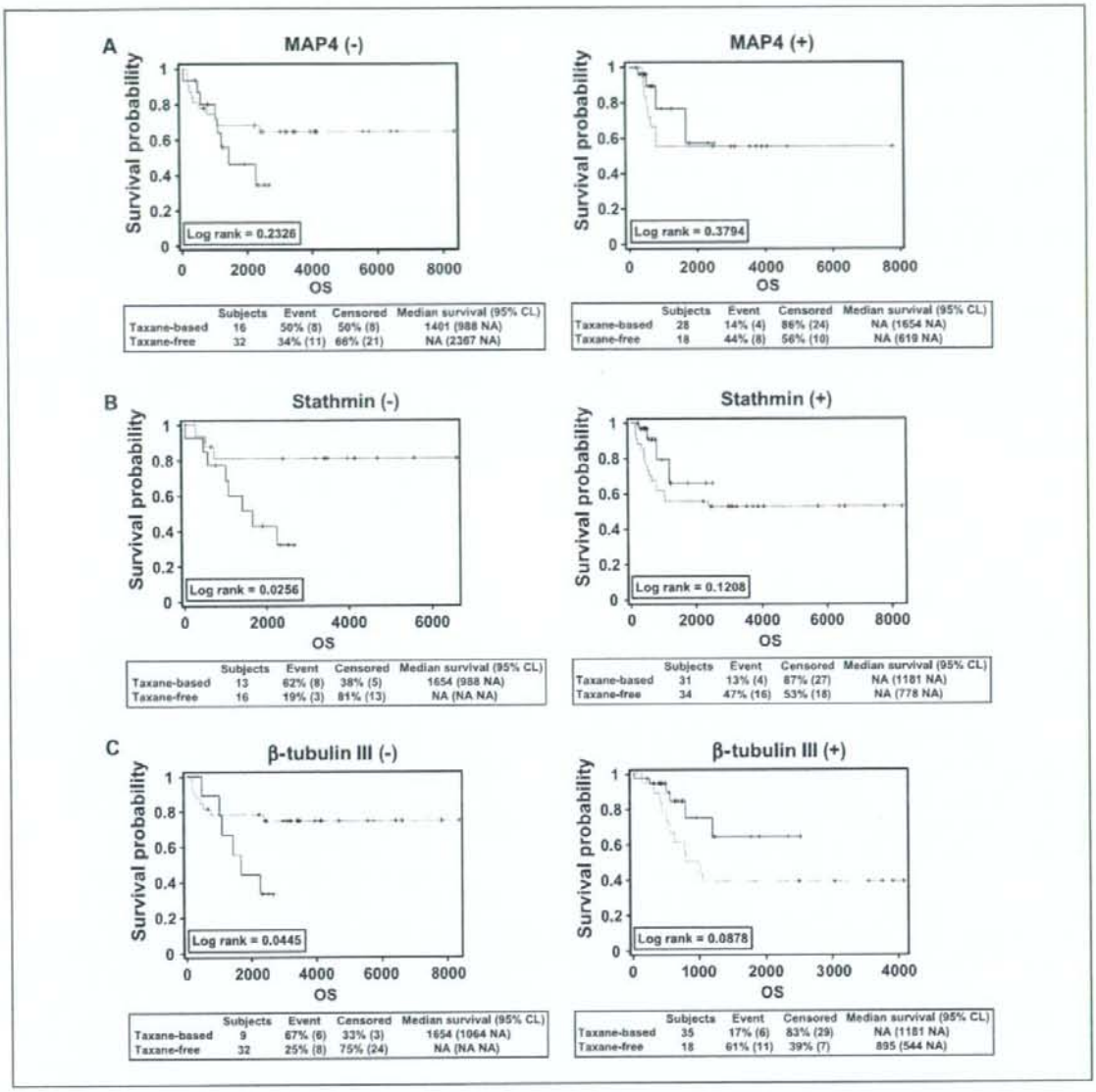

	Subjects	Event	Censored	Median survival (95% CL)
Taxane-based	16	50% (8)	50% (8)	1401 (988 NA)
Taxane-free	32	34% (11)	66% (21)	NA (2367 NA)

	Subjects	Event	Censored	Median survival (95% CL)
Taxane-based	28	14% (4)	86% (24)	NA (1654 NA)
Taxane-free	18	44% (8)	56% (10)	NA (619 NA)

	Subjects	Event	Censored	Median survival (95% CL)
Taxane-based	13	62% (8)	38% (5)	1654 (988 NA)
Taxane-free	16	19% (3)	81% (13)	NA (NA NA)

	Subjects	Event	Censored	Median survival (95% CL)
Taxane-based	31	13% (4)	87% (27)	NA (1181 NA)
Taxane-free	34	47% (16)	53% (18)	NA (778 NA)

	Subjects	Event	Censored	Median survival (95% CL)
Taxane-based	9	67% (6)	33% (3)	1654 (1064 NA)
Taxane-free	32	25% (8)	75% (24)	NA (NA NA)

	Subjects	Event	Censored	Median survival (95% CL)
Taxane-based	35	17% (6)	83% (29)	NA (1181 NA)
Taxane-free	18	61% (11)	39% (7)	895 (544 NA)

Fig. 3. The product-limit estimator of OS by regimens and microtubule-associated molecules. *A*, the product-limit estimators of OS for MAP4-negative patients (*left panel*) and for positive patients (*right panel*). *B*, the product-limit estimators of OS for stathmin-negative patients (*left panel*) and for positive patients (*right panel*). *C*, the product-limit estimators of OSfor β-tubulin III negative patients (*left panel*) and for positive patients (*right panel*). Solid lines, survival functions of patients receiving the taxane-based regimen; broken line, taxane-free regimen.

was the effect of the interaction between treatment and marker. With the supposition that the effect of a taxane-based regimen for marker-negative patients equals *A* and that of the taxane-free regimen for positive patients equals *B*, the significance of the interaction shows that the effect of the taxane-based regimen for the marker-positive patients is greater than *A*+*B* (i.e., it is synergistic). Evidence of a synergistic effect indicates that the effect of taxane is dependent on the status of the marker, showing the marker plays an important role in the effect of taxane. The cutoff points that determined positive and negative for each marker were chosen by the Akaike's information criterion so that the Cox model fitted best to the data (30).

Results

Effects of reducing expression of β-tubulin isoforms, MAP4, and stathmin on drug sensitivity to paclitaxel and cisplatin in ovarian cancer cells. We first examined whether gene silencing of

Table 2. Summary of interaction terms for the Cox regression

	MAP4	Stathmin	β-tubulin III
OS			
Regression coefficient (95% CI)	-0.77 (-2.50 to 0.96)	-1.37 (-3.17 to 0.43)	-1.68 (-3.16 to 0.21)
P	0.383	0.135	0.026
PFS			
Regression coefficient (95% CI)	-0.40 (-1.91 to 1.12)	-0.85 (-2.43 to 0.72)	-1.52 (-2.90 to -0.15)
P	0.608	0.288	0.030

Abbreviation: 95% CI, 95% confidence interval.

β-tubulin isoforms, MAP4, and stathmin could affect drug sensitivity to paclitaxel and cisplatin in the cultured human ovarian cancer cell lines SKOV-3 and OVCAR-3. Cellular mRNA expression levels of these genes in two human ovarian cancer cell lines were all markedly down-regulated when treated with respective siRNA (Fig. 1A). We then examined the drug sensitivities of paclitaxel or cisplatin in ovarian cancer cells treated with siRNA of the tubulin isoforms, MAP4, and stathmin (Fig. 1B). When β-tubulin III or β-tubulin IV was silenced, the IC_{50} values of paclitaxel increased to 16.8 nmol/L and 14.3 nmol/L, respectively, from the control IC_{50} value of 3.9 nmol/L in SKOV-3 cells (Fig. 1B). By contrast, down-regulation of β-tubulins I and II, MAP4, and stathmin did not influence the sensitivity to paclitaxel in SKOV-3 cells. Down-regulation of β-tubulins I, II, III, and IV, MAP4, and stathmin did not influence sensitivity to cisplatin in either cell line (Fig. 1B). Two independent experiments consistently showed the acquisition of drug resistance to paclitaxel in SKOV-3 by knockdown of β-tubulins III and IV.

Immunohistochemistry of MAP4, stathmin, and β-tubulin III in human ovarian clear cell adenocarcinomas. Clinical and pathologic characteristics at diagnosis are summarized in Supplementary Table S1. The median age of the patients was 52 years (range, 29-74 years). Sixty tumors were considered to be stage I, 7 stage II, 20 stage III, and 7 stage IV. Sixteen patients who had residual tumors more than 1 cm in maximum diameter were classified into the suboptimal group, whereas 78 patients were placed in the optimal group with a residual tumor ≤1 cm, including 74 complete resections. The median follow-up for PFS for all 94 patients was 749 days (range, 23-8,318 days), whereas the median follow-up for OS was 995 days (range, 23-8,318 days). The median follow-up of those patients who are currently progression-free is 2,399 days (range, 212-8,318 days).

Table 3. Hazard ratios (marker positive/marker negative) for subpopulations of taxane-based regimen and taxane-free regimen by the Cox proportional hazards models; two-tailed 95% confidence intervals are given in parenthesis

Marker hazard ratio (95% CI)	Taxane-based therapy	Taxane-free therapy	*P*
Overall survival			
MAP4	0.42 (0.11-1.66)	0.91 (0.35-2.40)	0.383
Stathmin	0.96 (0.26-3.53)	3.78 (1.07-13.34)	0.135
β-tubulin III	0.72 (0.22-2.44)	3.91 (1.49-10.23)	0.026
Progression-free survival			
MAP4	0.53 (0.17 -1.69)	0.79 (0.31-2.02)	0.608
Stathmin	1.11 (0.36-3.41)	2.60 (0.85-7.96)	0.288
β-tubulin III	0.77 (0.26-2.31)	3.52 (1.37-9.01)	0.030

NOTE: Age, FIGO stage, peritoneal cytodianosis, and size of residual tumor were adjusted by the propensity scores representing the four covariates.
P values are based on Wald tests for interaction of taxane with the marker.

The cytoplasmic positive expression of MAP4 was detected in 46 tumors (49%). Positive immunostaining for stathmin was found in 54 tumors (57%), predominantly as cytoplasmic staining (Fig. 2A). β-Tubulin III immunostaining was positive in 53 (56%) tumors with total scores of 7 or 8 (Fig. 2C). Positive MAP4 and β-tubulin III expression was frequent in tumors treated with taxane-containing regimens, compared with tumors treated with taxane-free regimens (Supplementary Table S1). Stathmin-positive tumors were also more frequent in patients with the taxane-based regimen, although the difference failed to reach statistical significance. There were no measurable differences in immunoreactivities for these proteins with respect to either tumor stage or residual tumor (Table 1).

Effects of β-tubulin III expression on survival in human ovarian clear cell adenocarcinomas. In Fig. 3A, the product-limit estimators for OS of patients administered the taxane-free and taxane-based regimens are shown for the MAP4-negative group (*left panel*) and for the MAP4-positive group (*right panel*). The survival outcome seemed to be less favorable for the taxane-based regimen than for the taxane-free regimen in the MAP4-negative group, although the difference was not statistically significant ($P = 0.23$); there was no difference in survival between the two regimens in the MAP4-positive group ($P = 0.38$). Paclitaxel treatment was also associated with a poorer survival in the stathmin-negative patients ($P = 0.03$); there was a trend to a better survival in the group of stathmin-positive patients ($P = 0.12$), as shown in Fig. 3B.

Survival associated with paclitaxel treatment was more evidently differential based on β-tubulin III status. In the absence of β-tubulin III expression, survival was significantly shorter in patients with the taxane-based regimen compared with those with the taxane-free regimen ($P = 0.04$), and the opposite was the case in the presence of β-tubulin III expression ($P = 0.09$; Fig. 3C). Table 2 gives the estimates, confidence intervals, and *P* values for the hazard ratios of the interaction. The table shows that for β-tubulin III, *P* values were 0.026 for OS and 0.030 for PFS. Thus, β-tubulin III seems to determine the efficacy of the taxane-based regimen. Table 2 also shows that for stathmin, *P* was 0.135 and the hazard ratio was 0.25 (95% confidence interval, 0.04-1.53) for OS, and 0.288 and 0.43, respectively (95% confidence interval, 0.09-2.06), for PFS.

Thus, stathmin may also determine the efficacy of the taxane-based regimen, but the effect was not statistically significant. Furthermore, Table 2 shows that for MAP4, the estimated hazard ratios were far from 1 but were not statistically significant (0.383 for OS and 0.673 for PFS).

The statistical significance of the interaction of taxane with β-tubulin III shown in Table 2 indicates that the efficacy of taxane depends on β-tubulin III positivity or negativity. To interpret this interaction precisely, we give the hazard ratio of the taxane-based regimen relative to the taxane-free regimen separately for β-tubulin III–positive and -negative patients. Table 3 gives the hazard ratios for patients who were positive for β-tubulin III relative to patients who were negative; these ratios are given separately for the taxane-based and taxane-free regimens. The table shows that the hazard ratio for OS was 3.91 for the taxane-free regimen but was 0.72 for the taxane-based regimen. This outcome indicates that being positive for β-tubulin III is related to a poor prognosis in the taxane-free regimen group, but that the taxane-based regimen may prolong OS for patients who are β-tubulin III–positive.

Discussion

Class III β-tubulin overexpression has been reported to be a marker of poor clinical outcome in patients with advanced ovarian cancer mainly containing serous type adenocarcinoma. With treatment using platinum/paclitaxel therapy (16), expression of class III β-tubulin also predicts response and outcome in patients with non–small cell lung cancer and in those with breast cancer who are treated with taxane-based chemotherapy (31, 32). In this study, we investigated which targets could be responsible for the therapeutic efficacy of taxane-based chemotherapy against ovarian clear cell adenocarcinoma patients when treated with either cisplatin/cyclophosphamide or cisplatin/taxane. Immunohistochemical staining was done for the surgically resected specimens using antibodies against class III β-tubulin, MAP4, and stathmin. Of these three targeting molecules, expression of class III β-tubulin was significantly associated with therapeutic efficacy of taxane-based chemotherapy, but not with taxane-free chemotherapy. Moreover, our present study showed that increased expression of class III β-tubulin significantly affected outcome for patients with ovarian clear cell adenocarcinoma in the taxane-treated patient group.

Our present finding is not consistent with those of previous studies identifying a close association of class III β-tubulin overexpression with poor therapeutic efficacy of taxane-based chemotherapy against ovarian cancers, including most non–clear cell adenocarcinomas (14–16). Of β-tubulin isoforms, microtubules containing tubulin III or IV were more dynamic and less stable than microtubules containing other tubulin types (13, 33), suggesting that cellular expression of β-tubulin isotype III or IV plays a critical role in drug sensitivity to paclitaxel *in vitro*. Paclitaxel-selected drug-resistant cancer cell lines derived from human lung, breast, pancreas, and prostate cancers and glioblastoma often exhibit enhanced expression of β-tubulin III (34). Kavallaris et al. have previously reported increased mRNA expression of β-tubulins III and IV in taxane-treated ovarian tumor samples as compared with primary untreated ovarian tumors (35). However, Nicolletti et al. have reported no correlation between tubulin expression and paclitaxel sensitivity in mouse xenografts of human ovarian carcinomas (36).

In our present study, knockdown of class III and IV β-tubulin genes but not of other tubulin isoforms specifically decreased drug sensitivity to paclitaxel in one ovarian cancer cell line, indicating the possible involvement of these tubulin isoforms in the dynamics of microtubules. At present, it remains unclear why decreased expression of type III β-tubulin differentially modulates drug sensitivity to paclitaxel among various cancer cell lines *in vitro*, and this finding requires further study. A complex network system among microtubule-related factors, including tubulin isoforms, operates in limiting drug sensitivity to taxanes; however, the results of our present study together with those of previous reports could present a novel notion that expression levels of class III β-tubulin might thus predict the therapeutic efficacy of taxane-based therapy. This effect would depend on differences in pathologic subtype between serous adenocarcinoma and clear cell adenocarcinoma.

We also found that OS of patients with lower expression of MAP4, stathmin, and β-tubulin indicated better therapeutic efficacy with non–taxane-based chemotherapy compared with taxane-based treatment. In patients with higher expression of stathmin and MAP4, these relationships were reversed but not statistically significant. Although these appeared during follow-up periods of the taxane-based therapy group for as long as 3,000 days, low expression of these three targeting molecules might predict poor prognosis for patients with ovarian clear cell adenocarcinoma.

Altered expression of proteins that regulate microtubule dynamics also mediates paclitaxel resistance in cancer cells *in vitro* through interaction with tubulin dimers or polymerizing microtubules. These proteins include stathmin, a microtubule destabilizer, and MAP4, a microtubule stabilizer (34). Altered expression of stathmin (5, 6) and MAP-4 (37) induces marked changes in drug sensitivity of cancer cells to taxanes. Further study is required to understand whether the above mechanisms *in vitro* underlie the poor therapeutic efficacy of taxane-based chemotherapy for patients with low expression of stathmin and MAP4, as well as β-tubulin. On the other hand, increased expression of stathmin also was associated (but not significantly) with an improved therapeutic efficacy of taxane-based chemotherapy in comparison with that of taxane-free therapy. Further study with a larger number of patients as well as longer follow-up periods may predict whether stathmin can be a marker for therapeutic efficacy of taxane-based therapy against ovarian clear cell adenocarcinoma.

In conclusion, our present study showed that overexpression of type III β-tubulin was a predictive marker of better prognosis for patients with ovarian clear cell adenocarcinoma when they are treated with taxane-based chemotherapy. This finding is not consistent with those involving patients with other serous type carcinoma treated by taxane-based chemotherapy, suggesting that association of β-tubulin expression with therapeutic efficacy by taxane-based chemotherapy depends on the pathologic characteristics of ovarian cancer.

Disclosure of Potential Conflicts of Interest

No potential conflicts of interest were disclosed.

References

1. Jordan MA. Mechanism of action of antitumor drugs that interact with microtubules and tubulin. Curr Med Chem Anti-Canc Agents 2002;2:1–17.
2. Drukman S, Kavallaris M. Microtubule alterations and resistance to tubulin-binding agents. Int J Oncol 2002; 21:621–8.
3. Maccioni RB, Cambiazo V. Role of microtubule-associated proteins in the control of microtubule assembly. Physiol Rev 1995;75:835–64.
4. Chapin SJ, Lue CM, Yu MT, Bulinski JC. Differential expression of alternatively spliced forms of MAP4: a repertoire of structurally different microtubule-binding domains. Biochemistry 1995;34:2289–301.
5. Balachandran R, Welsh MJ, Day BW. Altered levels and regulation of stathmin in paclitaxel-resistant ovarian cancer cells. Oncogene 2003;22:8924–30.
6. Alli E, Bash-Babula J, Yang JM, Hait WN. Effect of stathmin on the sensitivity to antimicrotubule drugs in human breast cancer. Cancer Res 2002;62: 6864–9.
7. Schiff PB, Fant J, Horwitz SB. Promotion of microtubule assembly *in vitro* by taxol. Nature 1979;277: 665–7.
8. Manfredi JJ, Parness J, Horwitz SB. Taxol binds to cellular microtubules. J Cell Biol 1982;94:688–96.
9. Rowinsky EK, Donehower RC. Paclitaxel (taxol). N Engl J Med 1995;332:1004–14.
10. McGuire WP, Hoskins WJ, Brady MF, et al. Cyclophosphamide and cisplatin compared with paclitaxel and cisplatin in patients in patients with stage III and stage IV ovarian cancer. N Engl J Med 1996;334:1–6.
11. Piccart MJ, Bertelsen K, James K, et al. Randomized intergroup trial of cisplatin-paclitaxel versus cisplatin-cyclophosphamide in women with advanced epithelial ovarian cancer: three-year results. J Natl Cancer Inst 2000;92:699–708.
12. International Collaborative Ovarian Neoplasm Group. Paclitaxel plus carboplatin versus standard chemotherapy with either single-agent carboplatin or cyclophosphamide, doxorubicin, and cisplatin in women with ovarian cancer: the ICON3 randomised trial. Lancet 2002;360:505–15.
13. Derry WB, Wilson L, Khan IA, Luduena RF, Jordan MA. Taxol differentially modulates the dynamics of microtubules assembled from unfractionated and purified β-tubulin isotypes. Biochemistry 1997;36: 3554–62.
14. Ferlini C, Raspaglio G, Mozzetti S, et al. The secotaxane IDN5390 is able to target class III β-tubulin and to overcome paclitaxel resistance. Cancer Res 2005;65:2397–405.
15. Mozzetti S, Ferlini C, Concolino P, et al. Class III β-tubulin overexpression is a prominent mechanism of paclitaxel resistance in ovarian cancer patients. Clin Cancer Res 2005;11:298–305.
16. Ferrandina G, Zannoni GF, Martinelli E, et al. Class III β-tubulin overexpression is a marker of poor clinical outcome in advanced ovarian cancer patients. Clin Cancer Res 2006;12:2774–9.
17. Scully RE. Tumors of the ovary and maldeveloped gonads. 3rd series. Washington (DC): Armed Forced Institute of Pathology; 1996. p. 141.
18. Seidman JD, Russell P, Kurman RJ. Surface epithelial tumors of the ovary. In: Blaustein A, Kurman RJ. Blaustein's pathology of the female genital tract. 5th ed. New York: Springer-Verlag; 2002. p. 873.
19. Shimizu M, Nikaido T, Toki T, Shiozawa T, Fujii S. Clear cell carcinoma has an expression pattern of cell cycle regulatory molecules that is unique among ovarian adenocarcinomas. Cancer 1999;85:669–77.
20. Ozols RF, Bundy BN, Greer BE, et al. Phase III trial of carboplatin and paclitaxel compared with cisplatin and paclitaxel in patients with optimally resected stage III ovarian cancer: a Gynecologic Oncology Group study. J Clin Oncol 2003;21:3194–200.
21. Sugiyama T, Kamura T, Kigawa J, et al. Clinical characteristics of clear cell carcinoma of the ovary. Cancer 2000;88:2584–9.
22. Pectasides D, Fountzilas G, Aravantinos G, et al. Advanced stage clear-cell epithelial ovarian cancer: the Hellenic Cooperative Oncology Group experience. Gynecol Oncol 2006;102:285–91.
23. du Bois A, Lück HJ, Meier W, et al. A randomized clinical trial of cisplatin/paclitaxel versus carboplatin/paclitaxel as first-line treatment of ovarian cancer. J Natl Cancer Inst 2003;95:1320–9.
24. International Federation of Gynecology and Obstetrics. Changes in definitions of clinical staging for cancer of the cervix and ovary. Am J Obstet Gynecol 1987;156:236–41.
25. Yuan RH, Jeng YM, Chen HL, et al. Stathmin overexpression cooperates with p53 mutation and osteopontin overexpression, and is associated with tumour progression, early recurrence, and poor prognosis in hepatocellular carcinoma. J Pathol 2006;209: 549–58.
26. Allred DC, Harvey JM, Berardo M, Clark GM. Prognostic and predictive factors in breast cancer by immunohistochemical analysis. Mod Pathol 1998;11: 155–68.
27. Ohishi Y, Oda Y, Basaki Y, et al. Expression of β-tubulin isotypes in human primary ovarian carcinoma. Gynecol Oncol 2007;105:586–92.
28. Rosenbaum PR, Rubin DB. The central role of the propensity score in observational studies for causal effects. Biometrika 1983;70:41–55.
29. Rosenbaum PR, Rubin DB. Reducing bias in observational studies using subclassification on the propensity score. J Am Stat Assoc 1984;79:516–24.
30. Akaike H. "A new look as the statistical model identification." IEEE Trans Autom Contr 1974;19:716–23.
31. Sève P, Mackey J, Isaac S, et al. Class III β-tubulin expression in tumor cells predicts response and outcome in patients with non-small cell lung cancer receiving paclitaxel. Mol Cancer Ther 2005;4:2001–7.
32. Paradiso A, Mangia A, Chiriatti A, et al. Biomarkers predictive for clinical efficacy of taxol-based chemotherapy in advanced breast cancer. Ann Oncol 2005; 16:14–9.
33. Panda D, Miller HP, Banerjee A, Luduena RF, Wilson L. Microtubule dynamics *in vitro* are regulated by the tubulin isotype composition. Proc Natl Acad Sci U S A 1994;91:11358–62.
34. Orr GA, Verdier-Pinard P, McDaid H, Horwitz SB. Mechanisms of Taxol resistance related to microtubules. Oncogene 2003;22:7280–95.
35. Kavallaris M, Kuo DY, Burkhart CA, et al. Taxol-resistant epithelial ovarian tumors are associated with altered expression of specific β-tubulin isotypes. J Clin Invest 1997;100:1282–93.
36. Nicoletti MI, Valoti G, Giannakakou P, et al. Expression of β-tubulin isotypes in human ovarian carcinoma xenografts and in a sub-panel of human cancer cell lines from the NCI-Anticancer Drug Screen: correlation with sensitivity to microtubule active agents. Clin Cancer Res 2001;7:2912–22.
37. Zhang CC, Yang JM, Bash-Babula J, et al. DNA damage increases sensitivity to vinca alkaloids and decreases sensitivity to taxanes through p53-dependent repression of microtubule-associated protein 4. Cancer Res 1999;59:3663–70.

Expression of HER2 and Estrogen Receptor α Depends upon Nuclear Localization of Y-Box Binding Protein-1 in Human Breast Cancers

Teruhiko Fujii,[1,3,5] Akihiko Kawahara,[1,4] Yuji Basaki,[6] Satoshi Hattori,[2] Kazutaka Nakashima,[1,4] Kenji Nakano,[1] Kazuo Shirouzu,[3] Kimitoshi Kohno,[7] Takashi Yanagawa,[2] Hideaki Yamana,[1,3] Kazuto Nishio,[8] Mayumi Ono,[6] Michihiko Kuwano,[1] and Masayoshi Kage[1,4]

[1]Center for Innovative Cancer Therapy of the 21st Century Center of Excellence Program for Medical Science; [2]Biostatistics Center, Kurume University; [3]Department of Surgery, Kurume University School of Medicine; [4]Department of Pathology, Kurume University Hospital, Kurume, Japan; [5]National Hospital Organization Kyushu Medical Cancer; [6]Department of Pharmaceutical Oncology, Graduate School of Pharmaceutical Sciences, Kyushu University, Fukuoka, Japan; [7]Department of Molecular Biology, University of Occupation and Environmental Health, Kitakyushu, Japan; and [8]Department of Genome Biology, Kinki University School of Medicine, Osakasayama, Japan

Abstract

In our present study, we examined whether nuclear localization of Y-box binding protein-1 (YB-1) is associated with the expression of epidermal growth factor receptors (EGFR), hormone receptors, and other molecules affecting breast cancer prognosis. The expression of nuclear YB-1, clinicopathologic findings, and molecular markers [EGFR, HER2, estrogen receptor (ER)α, ERβ, progesterone receptor, chemokine (C-X-C motif) receptor 4 (CXCR4), phosphorylated Akt, and major vault protein/lung resistance protein] were immunohistochemically analyzed. The association of the expression of nuclear YB-1 and the molecular markers was examined in breast cancer cell lines using microarrays, quantitative real-time PCR, and Western blot analyses. Knockdown of YB-1 with siRNA significantly reduced EGFR, HER2, and ERα expression in ERα-positive, but not ERα-negative, breast cancer cell lines. Nuclear YB-1 expression was positively correlated with HER2 ($P = 0.0153$) and negatively correlated with ERα ($P = 0.0122$) and CXCR4 ($P = 0.0166$) in human breast cancer clinical specimens but was not correlated with EGFR expression. Nuclear YB-1 expression was an independent prognostic factor for overall ($P = 0.0139$) and progression-free ($P = 0.0280$) survival. In conclusion, nuclear YB-1 expression might be essential for the acquisition of malignant characteristics via HER2-Akt–dependent pathways in breast cancer patients. The nuclear localization of YB-1 could be an important therapeutic target against not only multidrug resistance but also tumor growth dependent on HER2 and ERα. [Cancer Res 2008;68(5):1504–12]

Introduction

Nuclear localization of Y-box binding protein-1 (YB-1) is required for its transcriptional control of multidrug resistance–related genes and for its action in repairing DNA damage induced by anticancer agents and radiation in cancer cells; as a result of these actions, it is responsible for the acquisition of global drug resistance to a wide range of anticancer agents (1, 2). Immunohistochemical analyses have shown that nuclear YB-1 localization is a target marker of intrinsic importance for global drug resistance in cancer (2). Bargou et al. (3) reported that nuclear localization of YB-1 was associated with P-glycoprotein expression in human primary breast cancers, and other immunohistochemical studies have shown an association between YB-1 and P-glycoprotein in osteosarcoma, synovial sarcoma, breast cancer, ovarian cancer, and prostate cancer (4–12). Fujita et al. (13) reported that the increase in P-glycoprotein expression when patients were treated with paclitaxel was accompanied by nuclear YB-1 localization in breast cancers.

Nuclear expression of YB-1 is often associated with poor prognosis in various human malignancies, including breast cancer (3, 6), ovarian cancer (8, 11), synovial sarcoma (5), and lung cancer (14). In a study using molecular profiling, Faury et al. (15) recently showed that overexpression of YB-1 is a novel prognostic target for pediatric glioblastoma; however, the intracellular localization of YB-1 was not determined. These clinical studies suggest the close involvement of YB-1 in the acquisition of global drug resistance (2); however, it remains unclear whether the association of YB-1 with poor prognosis is due to this effect, as YB-1 nuclear localization is also a prognostic marker irrespective of P-glycoprotein expression (8, 14, 16). This suggests that other factors affecting tumor growth, invasion, and metastasis could also be involved in the association of YB-1 with poor prognosis in malignant cancers (8, 14).

YB-1 gene induced the development of breast cancers of many histologic types in an experimental animal model (17), suggesting that YB-1 is oncogenic (18). YB-1 overexpression in human mammary epithelial cells induced epidermal growth factor (EGF)-independent growth by activating the EGF receptor (EGFR) pathway (18). Jurchott et al. (19) reported that nuclear localization of YB-1 was induced during G_1-S phase transition, accompanied by increased expression of cyclin A and B. These studies suggest a close link between YB-1 expression and the growth potential of breast cancer cells, which might contribute to poor prognosis. Wu and colleagues (20) established a close correlation between YB-1 expression and the expression of EGFR and HER2 in breast cancer patients ($n = 389$) using tumor tissue arrays. Knock-out of YB-1 in mice caused some embryonic lethality, severe growth retardation, and exencephaly (21, 22). Moreover, fibroblasts derived from YB-$1^{-/-}$ knockout embryos had slower growth rates than those from wild-type embryos, and failed to undergo morphologic transformation *in vitro* (22, 23). Sutherland et al. (24) have also shown that breast cancer cells with defective nuclear localization of YB-1 multiply slowly in monolayers and during anchorage-independent growth.

Note: Supplementary data for this article are available at Cancer Research Online (http://cancerres.aacrjournals.org/).

T. Fujii, A. Kawahara, Y. Basaki, and S. Hattori contributed equally to this work.

Requests for reprints: Masayoshi Kage, Department of Pathology, Kurume University Hospital, Kurume 830-0011, Japan. Phone: 81-942-31-7651; Fax: 81-942-31-7651; E-mail: masakage@med.kurume-u.ac.jp.

doi:10.1158/0008-5472.CAN-07-2362

Taken together, these findings suggest that YB-1 plays a key role in the expression of not only drug resistance–related genes but also cell growth–related genes.

In the present study, we determined whether nuclear YB-1 localization influenced the expression of growth factor and hormone receptors, EGFR, HER2, estrogen receptor (ER)α, and ERβ, in human breast cancers. In addition, we used molecular profiling to examine whether nuclear YB-1 localization affected the expressions of major vault protein/lung resistance protein (MVP/LRP), phosphorylated Akt (p-Akt), progesterone receptor (PgR), and chemokine (C_X_C motif) receptor 4 (CXCR4).

Materials and Methods

Cell lines, protein extraction, and immunoblotting. Human breast cancer cell lines, T-47D, MCF-7, KPL-1, MDA-MB231, and SKBR-3 were obtained from the American Type Culture Collection and were grown as described elsewhere (25). Anti–YB-1 was generated as described previously (26). Anti-EGFR and anti-PTEN antibodies were obtained from Cell Signaling Technology. Anti-HER2 was purchased from Upstate, Inc. Anti-ERα was obtained from Santa Cruz Biotechnology, Inc. Anti-CXCR4 was obtained from Abcam plc. Anti– glyceraldehyde-3-phosphate dehydrogenase (GAPDH) was purchased from Trevigen, Inc. Anti-MVP/LRP was a kind gift from Professor S. Akiyama (Kagoshima University, Kagoshima, Japan). LY294002 was obtained from Sigma Co. Trastuzumab was purchased from Chugai Pharmaceutical Company. Cells were lysed in cold protein extraction reagent (M-PER; Pierce) with protease inhibitors and phosphatase inhibitors. Nuclear and cytoplasmic fractions were prepared as described previously (27). Lysates were subjected to SDS-PAGE and blotted onto Immobilon membrane (Millipore Corp.). After transfer, the membrane was incubated with the primary antibody and visualized with secondary antibody coupled to horseradish peroxidase and Supersignal West Pico Chemiluminescent Substrate (Pierce). Bands on Western blots were analyzed densitometrically using Scion Image software (version 4.0.2; Scion Corp.).

Microarray analysis. The small interfering RNA (siRNA) corresponding to nucleotide sequences of YB-1 (5′-GGU UCC CAC CUU ACU ACA U-3′) was purchased from QIAGEN Inc. SiRNA duplexes were transfected using Lipofectamine and Opti-MEM medium (Invitrogen) according to the manufacturer's recommendations. Duplicate samples were prepared for microarray hybridization. Forty-eight hours after siRNA transfection, total RNA was extracted from cell cultures using ISOGEN (Nippon Gene Co. Ltd.). Two micrograms of total RNA were reverse transcribed using GeneChip 3′-Amplification Reagents One-Cycle cDNA Synthesis kit (Affymetrix, Inc.) and then labeled with Cy5 or Cy3. The labeled cRNA was applied to the oligonucleotide microarray (Human Genome U133 Plus 2.0 Array; Affymetrix). The microarray was scanned on a GeneChip Scanner3000, and the image was analyzed using a GeneChip Operating Software ver1.

Quantitative real-time PCR. RNA was reverse transcribed from random hexamers using avian myeloblastosis virus reverse transcriptase (Promega). Real-time quantitative PCR was performed using the Real-time PCR system 7300 (Applied Biosystems). In brief, the PCR amplification reaction mixtures (20 μL) contained cDNA, primer pairs, the dual-labeled fluorogenic probe, and Taq Man Universal PCR Master Mix (Applied Biosystems). The thermal cycle conditions included maintaining the reactions at 50°C for 2 min and at 95°C for 10 min, and then alternating for 40 cycles between 95°C for 15 s and 60°C for 1 min. The primer pairs and probe were obtained from Applied Biosystems. The relative gene expression for each sample was determined using the formula $2^{(-\delta\ Ct)} = 2^{(Ct\ (GAPDH)-Ct\ (target))}$, which reflected the target gene expression normalized to GAPDH levels.

Immunohistochemistry. Anti-EGFR, anti-HER2, anti-ERα, and anti-PgR were obtained from Ventana Medical Systems. Anti-CXCR4 was purchased from Prosci, Inc. Anti-MVP/LRP was obtained from Chemicon. Tissue sections were taken from 73 breast cancer patients who underwent radical surgery in the Department of Surgery, Kurume University Hospital, Japan, between 1993 and 1999. The 4-μm tissue sections were deparaffinized, and the slides were heated in a Cell Conditioning Solution buffer for 60 min at 100°C. The sections were stained using the BenchMark XT (IHC Automated System) and ChemMate ENVISION method (Dako Corporation). BenchMark XT was used for staining anti–YB-1, anti-ERα, anti-EGFR, anti-HER2, and anti-PgR. The ChemMate ENVISION method was used for immunochemical staining of anti-ERβ, anti–p-Akt, anti-CXCR4, and anti-MVP/LRP. The samples were viewed using an Olympus BX51 fluorescence microscope (Olympus). The extent of staining of YB-1, ERα, ERβ, and PgR proteins was classified based on the percentage of cells with strongly stained nuclei: ≥10% indicated that a gland was positive for YB-1, and ≤9% indicated that it was negative. EGFR and HER2 expressions were classified into four categories: score 0, no staining at all or membrane staining in <10% of tumor cells; score 1+, faint/barely perceptible partial membrane staining in >10% of tumor cells; score 2+, weak to moderate staining of the entire membrane in >10% of tumor cells; and score 3+, strong staining of the entire membrane in >10% of tumor cells. The extent of immunohistologic staining for EGFR was defined as follows: scores of 2+ or 3+ were regarded as positive, and scores of 0 or 1+ were regarded as negative. The extent of immunohistologic staining for HER2 was defined as follows: scores of 3+ were regarded as positive, and scores of 0 or 1+ or 2+ were regarded as negative. Immunohistochemical staining of p-Akt and CXCR4 was defined based on the percentage of cells with strong cytoplasmic staining as follows: ≥10% indicated that a gland was positive, whereas ≤9% indicated that it was negative. MVP/LRP staining was defined as follows: ≥50% of cells with a strongly stained cytoplasm indicated that a gland was positive, whereas ≤49% indicated that it was negative. All immunohistochemical studies were evaluated by two experienced observers who were blind to the conditions of the patients.

Statistical analysis. The associations between YB-1 and clinicopathologic findings (age, tumor size, menopausal status, histologic grade, and lymph node metastasis) and molecular markers were tested by Fisher's exact test, the χ^2 test, or the Wilcoxon rank-sum test, depending on the type of data. A P value of <0.05 was regarded as significant unless otherwise indicated. The relationships between YB-1 expression and overall survival/progression-free survival, as well as other clinicopathologic findings and molecular markers, were examined by the Kaplan-Meier method and the log-rank test. Hazard ratios (HR) were estimated by Cox regressions.

As YB-1 and the expression of receptors of the EGFR family and hormone receptors, as well as the clinicopathologic findings, were all correlated, we summarized them by means of their principal components and investigated the relationship between these components and overall survival/progression-free survival by Cox regression. The relationship between the principal components was found to be related to overall survival/progression-free survival, and the clinicopathologic findings and molecular markers were investigated by studying their correlations. In addition, to obtain a direct representation of the relationship between molecular markers, we used a graphical modeling technique incorporating logistic regressions; a path was drawn between two markers only if these markers were conditionally associated with a significance level of 0.1, given the other markers. The data on overall survival and progression-free survival in this analysis were updated on February 27, 2007.

Results

The knock-down of YB-1 alters the expression of EGFR, HER2, ERα, CXCR4, and MVP/LRP genes. We initially compared the expressions of YB-1 siRNA–treated and control MCF-7 breast cancer cells using a high-density oligonucleotide microarray. Of the 54,675 RNA transcripts and variants in the microarray, we identified differentially expressed genes containing 43 genes that were up-regulated >2-fold and 203 genes that were down-regulated 0.5-fold or less (Supplementary Table S1). It has been reported that the activity of PI3K/Akt was required for translocation of YB-1 into the nucleus (24, 27). We therefore investigated the effect of LY294002, a selective inhibitor of PI3K, in both T-47D and MDA-MB231 cells. LY294002 inhibited the

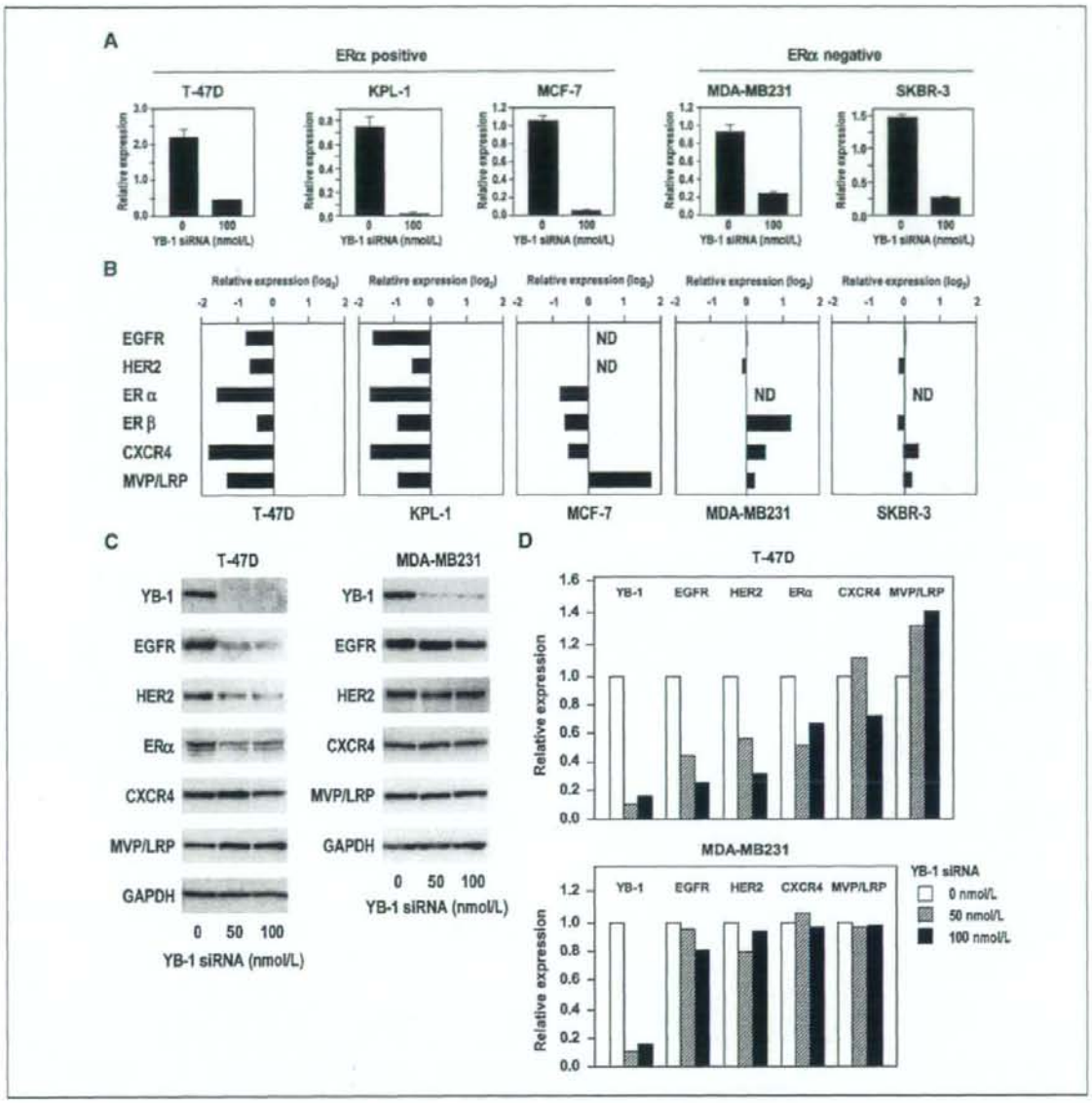

Figure 1. Effect of YB knock-down on expression of EGFR, HER2, ERα, CXCR4, and MVP/LRP in ERα-positive and ERα-negative breast cancer cells. *A*, YB-1 knock-down by treatment of YB-1 siRNA for 48 h. Relative mRNA expression was measured by qRT-PCR. *Columns*, mean of three independent experiments; *bars*, SD. *B*, levels of EGFR, HER2, ERα, ERβ, PgR, CXCR4, and MVP/LRP mRNA expression in YB-1 siRNA–treated cells. Changes of mRNA expression were expressed as the log of relative expression. *ND*, not detected. *C*, T-47D and MDA-MB231 cells were incubated with YB-1 siRNA for 72 h, and lysates were prepared. *D*, levels of YB-1, EGFR, HER2, ERα, CXCR4, and MVP/LRP expression were measured by densitometry.

nuclear expression of YB-1 in both cell lines (Supplementary Fig. S1*A*), consistent with previous reports (24, 27). We also examined whether PTEN status was correlated with nuclear YB-1 expression in breast cancer cells. Of the five human breast cancer cell lines used, cellular levels of the PTEN were not significantly correlated with nuclear expression levels of YB-1 protein (Supplementary Fig. S1*B* and *C*).

The differentially expressed genes included MVP/LRP and CXCR4, consistent with our previous study on human ovarian cancer cells (27). We next tested, by quantitative real-time PCR (qRT-PCR), whether the expression of CXCR4 and MVP/LRP was affected by knock-down of YB-1 in various human breast cancer cell lines. We also examined the expressions of growth factor receptors and hormone receptors, such as EGFR, HER2, ERα, and